

# MouseGPT: A Large-scale Vision-Language Model for Mouse Behavior Analysis

Teng Xu<sup>1,2†</sup>, Taotao Zhou<sup>1,2†</sup>, Youjia Wang<sup>1,2†</sup>, Peng Yang<sup>3†</sup>,  
Simin Tang<sup>3</sup>, Kuixiang Shao<sup>1</sup>, Zifeng Tang<sup>3</sup>, Yifei Liu<sup>1</sup>,  
Xinyuan Chen<sup>3</sup>, Hongshuang Wang<sup>4</sup>, Xiaohui Wang<sup>5</sup>,  
Huoqing Luo<sup>3</sup>, Jingya Wang<sup>1</sup>, Ji Hu<sup>3\*</sup>, Jingyi Yu<sup>1\*</sup>

<sup>1\*</sup>School of Information Science and Technology, ShanghaiTech University, 201210, Shanghai, China.

<sup>2</sup>LumiAni Technology, 201210, Shanghai, China.

<sup>3</sup>School of Life Science and Technology, ShanghaiTech University, 201210, Shanghai, China.

<sup>4</sup>Laboratory of Chemical Biology, Changchun Institute of Applied Chemistry, Chinese Academy of Sciences, Changchun, 130022, Jilin, China.

<sup>5</sup>School of Applied Chemistry and Engineering, University of Science and Technology of China, Hefei, 230026, Anhui, China.

\*Corresponding author(s). E-mail(s): [huji@shanghaitech.edu.cn](mailto:huji@shanghaitech.edu.cn);  
[yujingyi@shanghaitech.edu.cn](mailto:yujingyi@shanghaitech.edu.cn);

Contributing authors: [xt@shanghaitech.edu.cn](mailto:xt@shanghaitech.edu.cn);  
[zhoutt2023@shanghaitech.edu.cn](mailto:zhoutt2023@shanghaitech.edu.cn); [wangyj2@shanghaitech.edu.cn](mailto:wangyj2@shanghaitech.edu.cn);  
[yp@shanghaitech.edu.cn](mailto:yp@shanghaitech.edu.cn); [tangsm2023@shanghaitech.edu.cn](mailto:tangsm2023@shanghaitech.edu.cn);  
[shaokx@shanghaitech.edu.cn](mailto:shaokx@shanghaitech.edu.cn); [tangzf@shanghaitech.edu.cn](mailto:tangzf@shanghaitech.edu.cn);  
[arnoliu@shanghaitech.edu.cn](mailto:arnoliu@shanghaitech.edu.cn); [chenxy7@alumni.shanghaitech.edu.cn](mailto:chenxy7@alumni.shanghaitech.edu.cn);  
[hongshuang.wang@ciac.ac.cn](mailto:hongshuang.wang@ciac.ac.cn); [xiaohui.wang@ciac.ac.cn](mailto:xiaohui.wang@ciac.ac.cn);  
[luohq@shanghaitech.edu.cn](mailto:luohq@shanghaitech.edu.cn); [wangjingya@shanghaitech.edu.cn](mailto:wangjingya@shanghaitech.edu.cn);

<sup>†</sup>These authors contributed equally to this work.

## Abstract

Analyzing animal behavior is crucial in advancing neuroscience, yet quantifying and deciphering its intricate dynamics remains a significant challenge. Traditional machine vision approaches, despite their ability to detect spontaneous

behaviors, fall short due to limited interpretability and reliance on manual labeling, which restricts the exploration of the full behavioral spectrum. Here, we introduce MouseGPT, a Vision-Language Model (VLM) that integrates visual cues with natural language to revolutionize mouse behavior analysis. Built upon our first-of-its-kind dataset—incorporating pose dynamics and open-vocabulary behavioral annotations across over 42 million frames of diverse psychiatric conditions—MouseGPT provides a novel, context-rich method for comprehensive behavior interpretation. Our holistic analysis framework enables detailed behavior profiling, clustering, and novel behavior discovery, offering deep insights without the need for labor-intensive manual annotation. Evaluations reveal that MouseGPT surpasses existing models in precision, adaptability, and descriptive richness, positioning it as a transformative tool for ethology and for unraveling complex behavioral dynamics in animal models.

**Keywords:** behavior analysis, Vision-Language Model, Open-vocabulary

## 1 Introduction

Animal behavior studies have long been a cornerstone in systems neuroscience [1–3] and psychiatric research [4]. They provide a controlled, manipulable framework for modeling human neurological and psychiatric conditions in animals, enabling the investigation of neural and molecular mechanisms that may offer insights applicable to humans. Through genetic, chemical, and environmental manipulations, scientists can probe causative relationships, identify potential targets for psychiatric therapies, while providing valuable translational insights that facilitate drug testing. For example, the classic Tail Suspension Test (TST) [5, 6] and Forced Swim Test (FST) [6] help quantify behaviors in rodents [7] suggestive of depressive states by measuring immobility. Although simple and reproducible, such tests are short-term and do not reflect the complexity and chronic nature of depression. In reality, the behaviors of rodents are often subtle, fluctuating, and interrelated, spanning locomotion, grooming, social interactions, exploratory behavior, and responses to novel stimuli. Each of these behaviors can provide unique insights critical for modeling complex experimental conditions.

Capturing these behaviors across diverse experimental conditions typically relies on video recordings. These recordings then unanimously rely on human observers who need to watch whole experiment footage and count or note specific behaviors to derive statistical data [8]. This process is labor-intensive, prone to fatigue, bias, and inconsistency, and becomes especially challenging in advanced scenarios like free-moving or socially interacting mice. The immense volume and complexity of behavioral data further exacerbate the difficulty, often leading to selective recording that overlooks subtle but critical behaviors [9]. These limitations—compounded by subjective interpretation and the inability to document behaviors consistently in real-time—significantly undermine the accuracy and reliability of collected data [10–12].

Advancements in artificial intelligence have driven the development of automatic tools that mitigate the challenges of manual observation, with the goal to make

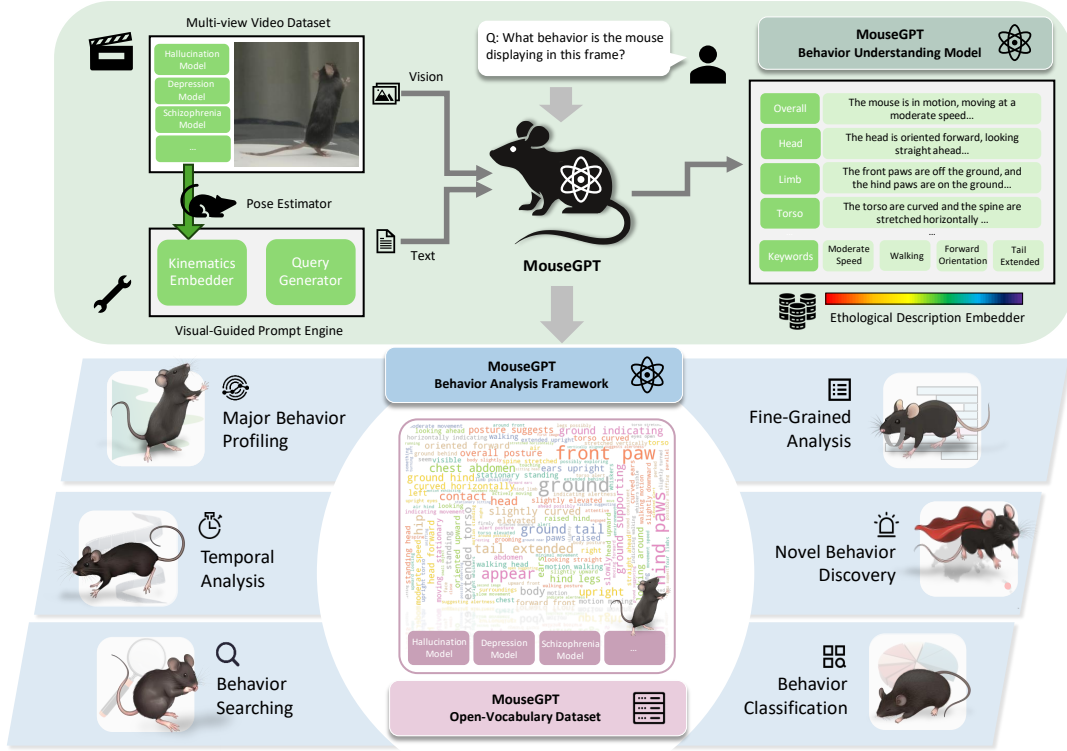


**Fig. 1** We present **MouseGPT**, a **comprehensive mouse behavior understanding model and analysis framework**. By integrating multi-view video data, pose estimation, and kinematic embeddings, MouseGPT generates open-vocabulary ethological descriptions of mouse behaviors. It leverages a visual-guided prompt engine and a pioneering open-vocabulary behavioral dataset, featuring disease-specific behavior phenotypes (e.g., hallucination, depression, schizophrenia). The system supports behavior classification, temporal analysis, fine-grained behavior profiling, and novel behavior discovery, delivering transformative capabilities for studying and analyzing complex animal behaviors.

behavior analysis more efficient and scalable. Supervised learning algorithms [13, 14] have shown success in automating the identification of specific, predefined behaviors, such as “vomiting” or “head-shaking”, by using expert-annotated datasets. In these approaches, researchers manually label behaviors in video or sensor data, creating training sets that enable recognition of unique movement patterns [15]. Once trained, they can classify target behaviors in new data quickly and with accuracy matching human experts. However, supervised techniques are only as good as the labeled datasets used to train them, requiring meticulous expert input to ensure reliability. Furthermore, they are inherently limited to recognizing behaviors they have been trained on, making them less adept at identifying novel or unexpected actions.

Latest unsupervised algorithms offer a distinct advantage in behavior analysis by identifying patterns without relying on predefined labels, thus enabling the discovery

of novel or unexpected behaviors. Techniques such as clustering and dimensionality reduction (e.g., t-SNE, PCA) analyze raw data to group similar actions without needing specific training examples. They leverage features like 3D keypoint positions [16–21], spatial-temporal attributes such as movement speed [22–24], and joint angles [19, 20] to group behaviors into clusters such as resting, grooming, or exploring, even in the absence of prior behavioral definitions, providing insights into complex neurological or mental states as well as addressing the issue of behavioral diversity. However, the effectiveness of unsupervised methods [25, 26] is often constrained by the quality of the selected features. For example, existing methods have predominantly relied on the kinematic ones [16, 27] and the resulting clusters may not readily reflect semantic meaningful behavioral distinctions [28, 29]. Moreover, subtle or rare behaviors are prone to being mis-clustered [30], requiring manual review for correction. To fully capture the complexities of mouse behavior, it is essential to have a universal feature — one that is robust, generalizable, and semantically rich.

Vision-Language Models (VLMs) provide a viable path to deliver the sought-after “universal feature”. By intertwining visual and textual data, VLMs offer a richer, more nuanced understanding of complex multi-modal tasks and have already proven effective in tackling challenges across diverse research domains [31–37]. Here, we introduce MouseGPT, a foundational VLM that links visual cues, such as postures or movements, with natural language annotations, to interpret animal behaviors beyond the limitations of predefined categories. Trained on large and diverse datasets, MouseGPT effectively generalizes to recognize subtle or novel actions, even those previously unseen, by identifying semantically similar patterns. This adaptability supports real-time, scalable annotation, offering contextually relevant descriptions that enrich behavioral analysis. By combining visual and linguistic elements, MouseGPT provides a structured yet adaptable tool, one that can accommodate the complexity and diversity inherent in mouse behavior studies, ultimately delivering a more insightful and flexible approach to understanding behavior.

MouseGPT advances mouse behavior research through three key contributions. First, it enables a comprehensive interpretation of mouse behaviors by integrating visual and textual information to generate detailed, context-sensitive descriptions. This approach captures behavioral nuances that traditional methods often overlook, providing a more robust and automated solution for studying complex behaviors. Second, we deliver a first-of-its-kind open-vocabulary dataset of over 42 million frames of multi-view video recordings, covering mice under various psychiatric conditions, including depression, hallucination, and schizophrenia. Unlike prior datasets that often lack sufficient scale and diversity, our dataset ensures a broad representation of behaviors, enhancing MouseGPT’s ability to deliver accurate and insightful behavioral analysis. Finally, we designed an integrated behavioral analysis framework that offers advanced tools for behavioral clustering, classification, and statistical assessment. By mapping textual descriptions to high-dimensional feature embeddings, this framework allows researchers to quantify and explore mouse behaviors with precision, accommodating both high-level behavioral trends and fine-grained analysis. Together, these components position MouseGPT as a transformative tool, providing researchers with



a flexible, content-rich approach to deciphering the complexities of mouse behavior and facilitating novel discoveries in neuropsychiatric research.

To demonstrate the capabilities of MouseGPT, we evaluated its performance on several datasets, including those focused on hallucination and other psychiatric conditions in mice. We applied MouseGPT to these datasets to perform a range of functions such as behavior profiling, clustering, fine-grained behavior analysis, and new behavior discovery. These tasks highlight MouseGPT’s ability to accurately interpret and categorize complex behaviors, even in challenging scenarios involving nuanced behavioral patterns. For instance, MouseGPT effectively distinguished between different degrees of depression in mice, identified characteristic behaviors associated with hallucination, and provided valuable insights into the effects of various psychiatric conditions.

In our evaluations, MouseGPT was compared with other open-source and proprietary visual-language models, including GPT-4o, InternVL2 [38], and MiniCPM-2.6 [39]. The results demonstrated that MouseGPT outperformed these models in both accuracy and depth of behavioral understanding, particularly in its ability to generalize across different contexts and generate contextually rich descriptions. These findings underscore the robustness and versatility of MouseGPT as an essential tool for ethological research.

## 2 Results

### 2.1 Overview of MouseGPT: A Behavior Understanding Model and An Analytical Framework

We present MouseGPT, a comprehensive mouse behavior understanding foundation model and analysis framework built on a large-scale Vision-Language Model (VLM). MouseGPT takes multi-view visual signals and kinematic data as inputs (Fig. 1a), precisely interpreting mouse behavior using an open-vocabulary approach to capture both common and subtle actions. MouseGPT uses natural language features (Methods) to interpret and analyze complex behaviors (Fig. 1b), including previously undefined actions, across diverse experimental conditions.

The core of MouseGPT model consists of a vision encoder and a large language model (LLM), which together process multi-view images of mouse behavior to generate natural language descriptions of behavior (Sec. 2.2). To develop MouseGPT, we began with open-source community models, InternVL2 [38] and MiniCPM-2.6 [39], pre-trained on diverse datasets, and specialized them through a Supervised Fine-Tuning (SFT) process using our domain-specific MouseGPT dataset towards mouse behavior understanding (Sec. 2.2). The curated MouseGPT dataset includes detailed pose estimations, kinematic information, and open-vocabulary behavior annotations, ensuring the model’s robustness and generalization across different contexts (Sec. 2.2). This SFT process enables MouseGPT to deliver high accuracy in interpreting behavior data, making it a valuable tool for ethological research and psychiatric disorder studies (Sec. 2.4).

The MouseGPT Behavior Analysis Framework builds on the outputs of the behavior understanding model, providing researchers with a comprehensive suite of tools for detailed behavior profiling and analysis (Sec. 2.3). By vectorizing textual descriptions

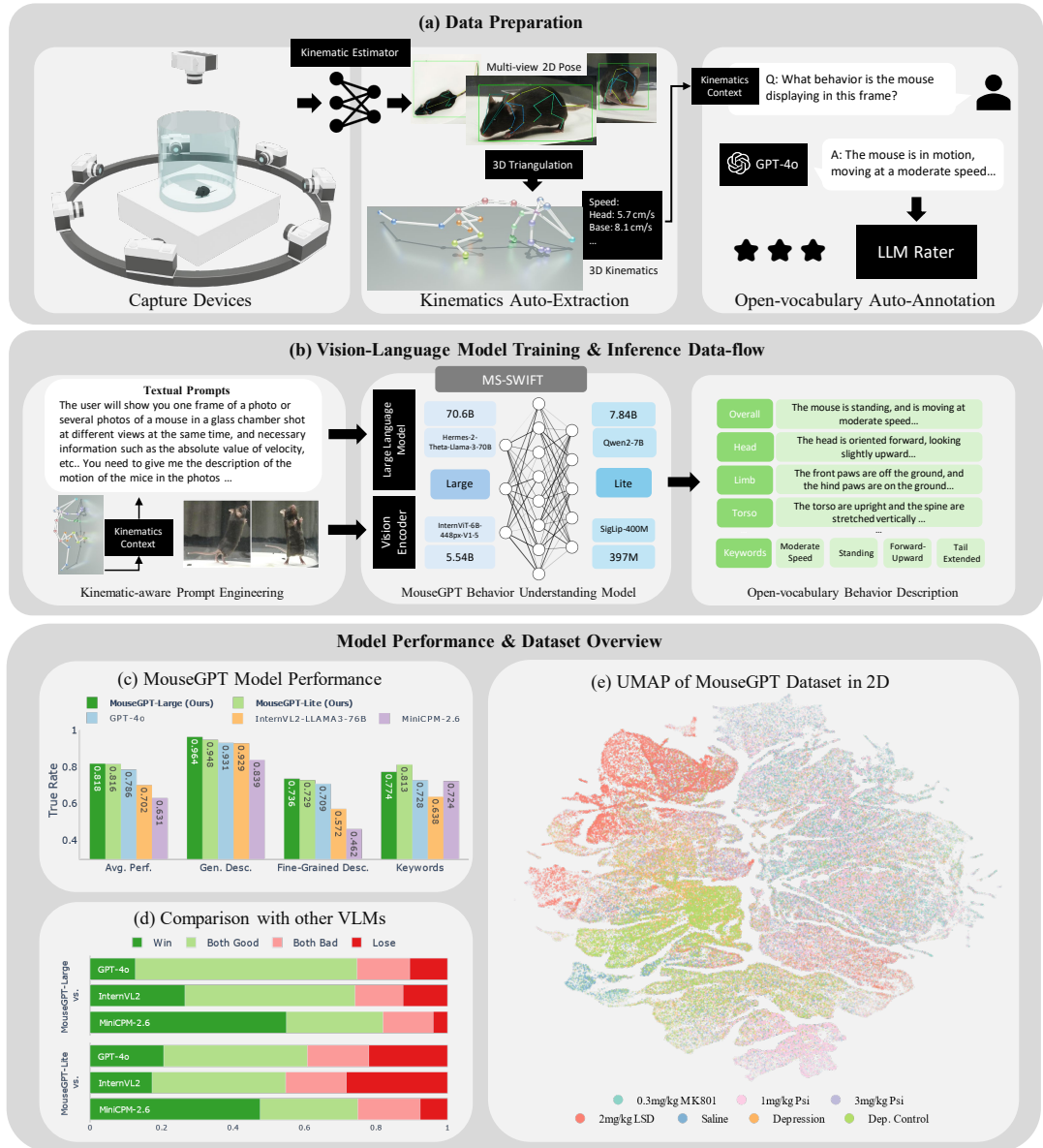


**Fig. 2 MouseGPT Behavior Understanding Model.** (a) Data Preparation: A multi-view 3D capture system generates keypoints and limb velocities for each frame, with training data produced by GPT-4o and refined through automated selection processes. (b) Vision-Language Model Training and Inference Workflow: MouseGPT-Large (70.6B parameters) is optimized for detailed behavior analysis, while MouseGPT-Lite (7.84B parameters) provides a lightweight alternative for streamlined tasks. (c) Performance Evaluation: Expert assessments highlight MouseGPT’s superior performance against open-source models of comparable size and GPT-4o in understanding mouse behavior. (d) Comparison with Other VLMs: Benchmarking against existing Vision-Language Models (VLMs) further demonstrates MouseGPT’s advanced capabilities, as rated by domain experts. (e) Dataset Visualization: UMAP projection of the MouseGPT dataset in 2D, with color-coded clusters representing distinct drug treatments.

using a high-dimensional text embedding model (Methods), MouseGPT captures the semantic nuances of each behavior. These vectorized representations allow researchers to explore behavior patterns through functionalities such as Major Behavior Profiling, Fine-Grained Behavior Analysis, Novel Behavior Discovery, and Behavioral Phenotype Prediction (Sec. 2.3).

Having established the platform that encompasses all the necessary steps for behavior quantification, we adopted a series of psychoactive substances to test whether MouseGPT could effectively capture the behavioral characteristics induced by different drugs (Sec. 2.4). By summarizing the continuous activities of the mice into a limited number of behavioral categories and comparing their proportions and spatiotemporal distributions, as well as conducting a more in-depth analysis of the sub-pattern within each category, we identified distinct behavioral profiles associated with each drug.

To enhance usability, we developed a Natural Language User Interface (NLUI) that allows seamless interaction with the model using extensive training data (Sec. 2.5). This chatbot-like interface enables researchers to interact with MouseGPT through natural language queries, simplifying tasks such as retrieving ethogram reports or performing behavior classification. The user-friendly design allows easy adaptation without extensive reprogramming, making MouseGPT an accessible and powerful tool for ethological research.

## 2.2 MouseGPT Enhances Mouse Behavior Understanding through Vision-Language Integration

MouseGPT addresses the challenges of comprehensive mouse behavior analysis by transforming vision signals captured by multi-view cameras into rich textual descriptions of mouse behaviors. Therefore, we developed and curated a comprehensive dataset, incorporating diverse behavior scenarios to enable effective supervised fine-tuning (SFT) and ensure robust model generalization.

The dataset was collected using a custom-built 3D video capture system comprising eight synchronized cameras capturing footage at 4K resolution and 60 frames per second (Fig. 2a-left, Methods). This setup provided precise, multi-angle recordings of mouse behaviors, which were then used to reconstruct accurate 3D key-point positions. (Fig. 2a-middle, Methods). These data were critical for capturing naturalistic and stimulus-induced behaviors, including conditions such as depression, hallucination, and schizophrenia, providing a diverse foundation for MouseGPT’s training. To further enhance the dataset quality, we employed an automated curation process using large language models (LLMs) (Fig. 2a-right, Methods). The annotations were rated automatically for quality by a rating model, allowing us to filter and retain only high-quality textual descriptions for model training.

To train and infer with MouseGPT, we employed a two-stage approach that involved kinematic-aware prompt engineering to generate enriched query prompts (Fig. 2b-left, Methods). These enriched prompts served as input during the SFT process of MouseGPT Vision-Language Model. The MS-SWIFT framework was used to facilitate training in multiple configurations (Methods), including MouseGPT-Large

(76 billion parameters) for high-accuracy applications and MouseGPT-Lite (8 billion parameters) for more computationally efficient tasks. This dual approach enables MouseGPT to adapt to a range of analytical and resource requirements.

The trained model outputs natural language descriptions of behaviors (Fig. 2b-right), which are then vectorized into high-dimensional embeddings [40] for downstream analysis (Sec. 2.3). To visualize the differences in behavior distribution across various experimental groups, we used Uniform Manifold Approximation and Projection (UMAP) [41] on the embeddings used by MouseGPT (Fig. 2e, Methods). The resulting UMAP plot exhibits clear clustering, with behaviors from different experimental groups represented by distinct colors, illustrating the model’s capability to distinguish behaviors between different conditions. These embeddings form the basis for a broad range of analysis capabilities, including behavioral clustering, classification, anomaly detection, and ethogram generation.

We benchmarked MouseGPT against other open-source models, including InternVL2, MiniCPM-2.6, and GPT-4o [42], and found that MouseGPT demonstrated superior performance in interpreting subtle and novel behaviors, as validated by domain experts (Fig. 2c,d). MouseGPT-Large achieved the highest accuracy for detailed behavior interpretation, while MouseGPT-Lite provided an efficient solution for computationally constrained environments. These evaluations highlight MouseGPT’s precision and versatility as a foundational tool for mouse behavior research.

### 2.3 Advanced Behavior Analysis Framework of MouseGPT

MouseGPT’s advanced framework begins by converting natural language descriptions of mouse behaviors into quantitative metrics (Fig. 3a), enabling a broad range of analytical techniques. By leveraging these open-vocabulary descriptions, MouseGPT offers a versatile approach to comprehensively analyze mouse behaviors, facilitating clustering of behavioral patterns (Fig. 3b), analysis of fine-grained behaviors (Fig. 3c), identification of novel activities (Fig. 3d), and prediction of behavioral phenotypes (Fig. 3e). This transformation from descriptive language to quantitative insights allows researchers to explore behavioral data with more detail and flexibility than traditional label-based methods.

The major behavior profiling capability of MouseGPT enables researchers to group similar behaviors based on their semantic descriptions through a two-stage LLM-guided clustering process (Fig. 3b). In the first stage, behaviors are clustered using Uniform Manifold Approximation and Projection (UMAP) and hierarchical clustering to create base clusters. (Methods) In the second stage, the LLM refines these clusters using additional contextual features, optimizing the clustering outcome. (Methods) This method allows behaviors to be grouped in an open-vocabulary manner, providing an intuitive overview of different behavior categories. For instance, applying this analysis to mice with depression-like conditions reveals distinct clusters such as “grooming”, “walking”, or “rearing”, each representing characteristic behaviors of different experimental groups. This profiling approach allows for adaptive analysis at multiple levels of granularity, enabling researchers to capture both broad behavioral trends and specific nuances.

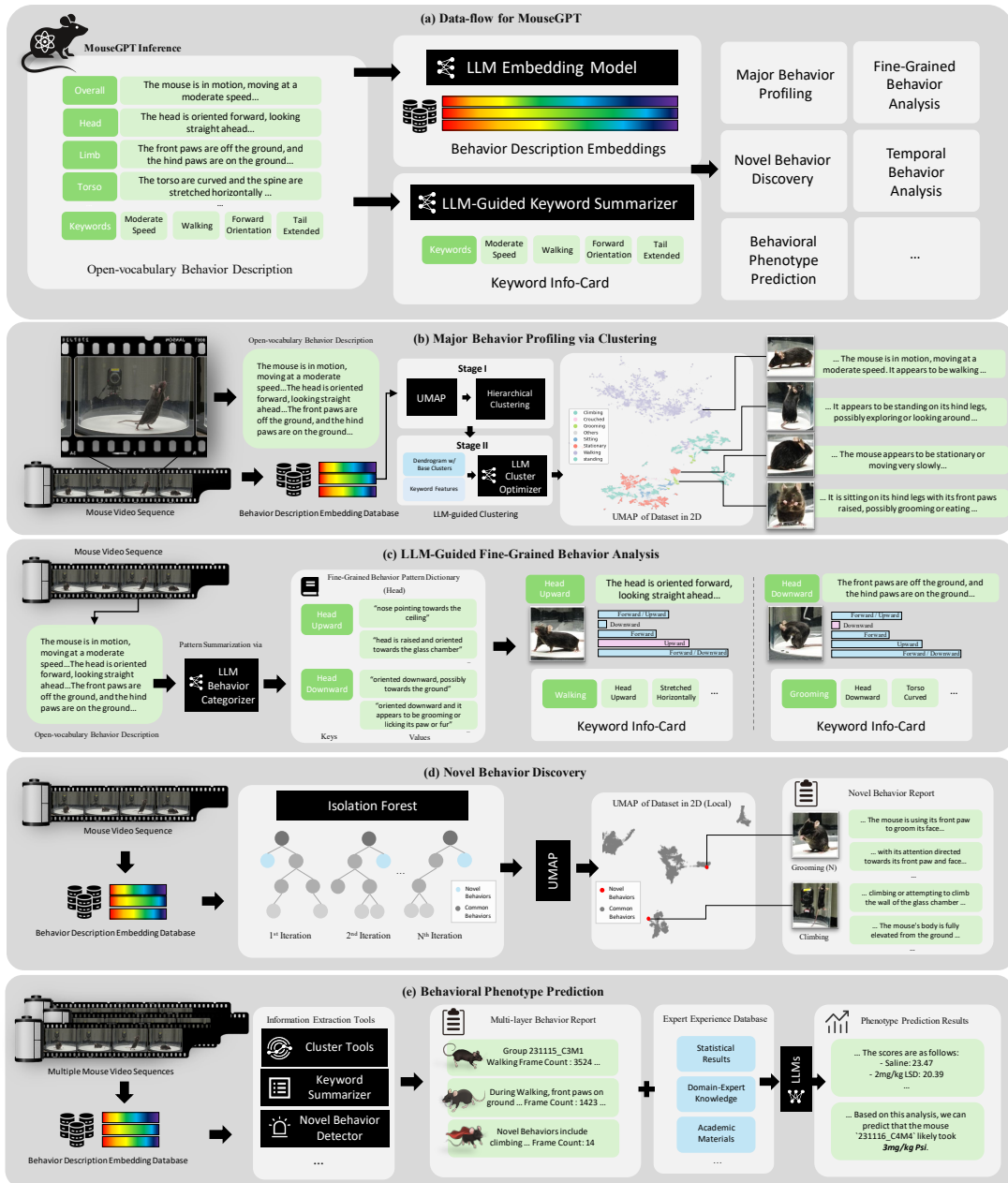


**Fig. 3 MouseGPT Behavior Analysis Framework.** (a) Data Flow: MouseGPT converts open-vocabulary behavior descriptions into two computable features: high-dimensional embeddings for semantic analysis and keyword-based summaries for interpretability, powering various downstream applications. (b) Major Behavior Profiling: A two-stage LLM-enhanced clustering groups mouse actions into distinct behavioral categories, with colors representing clusters, enabling robust profiling. (c) Fine-Grained Analysis: MouseGPT extracts and quantifies detailed behavior patterns via keyword analysis and frequency calculations, offering precise insights. (d) Novel Behavior Discovery: Using Isolation Forest in embedding space, MouseGPT identifies anomalous behaviors, visualized in 2D UMAP to highlight rare actions. (e) Phenotype Prediction: MouseGPT combines behavioral analysis with expert knowledge to predict drug treatments, aiding in phenotype understanding and experimental outcomes.

MouseGPT’s framework offers fine-grained behavior analysis (Fig. 3c), focusing on body-part level behaviors described in natural language, which provides additional detail by capturing specific actions and orientations of individual body parts. Using an LLM-guided categorization approach, MouseGPT constructs a pattern dictionary (Methods) that captures detailed behavioral characteristics at the body-part level, such as different head orientation, “head forward”, “head downward”, or limb movement, “forelimb in the air”, “forelimb on the ground”, etc. Each behavior is summarized with precise descriptions, which are then compiled into statistically analyzable keyword info-cards (Methods), offering a concise overview of the features and frequency of these fine-grained behaviors. This capability enables researchers to explore detailed and nuanced aspects of mouse activity, making it suitable for in-depth studies of behavior dynamics and their temporal evolution.

MouseGPT also excels in discovering novel behaviors by identifying outliers within the behavioral embedding space (Methods). Using an Isolation Forest algorithm (Methods), MouseGPT detects uncommon or previously unobserved behaviors across multiple iterations (Fig. 3d). These potential novel behaviors are then visualized using UMAP, allowing researchers to easily identify clusters of atypical activities. The identified behaviors are subsequently documented in novel behavior reports (Methods), offering detailed descriptions that help researchers investigate new behavioral phenotypes, particularly in experimental settings involving unknown variables, such as drug treatments or genetic modifications.

Finally, MouseGPT incorporates a behavioral phenotype prediction module that uses insights from various behavior analysis techniques to predict underlying phenotypic traits (Fig. 3e, Methods). The system aggregates information from clustering results, fine-grained behavior analysis, and novel behavior detection, producing a multi-layer behavior report (Methods). This report is then combined with an expert experience database, which includes statistical findings, domain-expert knowledge, and relevant academic materials, to refine phenotype predictions (Methods). Using a large language model, MouseGPT effectively synthesizes the gathered behavioral data and expert insights to predict potential phenotypes of the subjects. This approach provides researchers with a data-driven mechanism to link observed behaviors to corresponding biological conditions, aiding in studies of neuropsychiatric disorders and other complex biological phenomena.

## 2.4 MouseGPT Differentiates Behavioral Patterns in Mice Under Various Psychoactive Drugs

In order to demonstrate the capability of MouseGPT in revealing patterns and internal structures of behaviors, MouseGPT was used to analyze the behavioral changes of mice under the intervention of a series of psychoactive drugs. We employed two classic psychedelics Psilocybin (Psi) and Lysergic Acid Diethylamide (LSD), as well as MK801, which is frequently used to induce schizophrenia in mice. All of these drugs are capable of inducing hallucinatory responses in mice; however, the specific differences remain to be elucidated.

Recordings were initiated immediately after acute drug administration in mice, and the collected data were subjected to 3D skeletal reconstruction and semantic



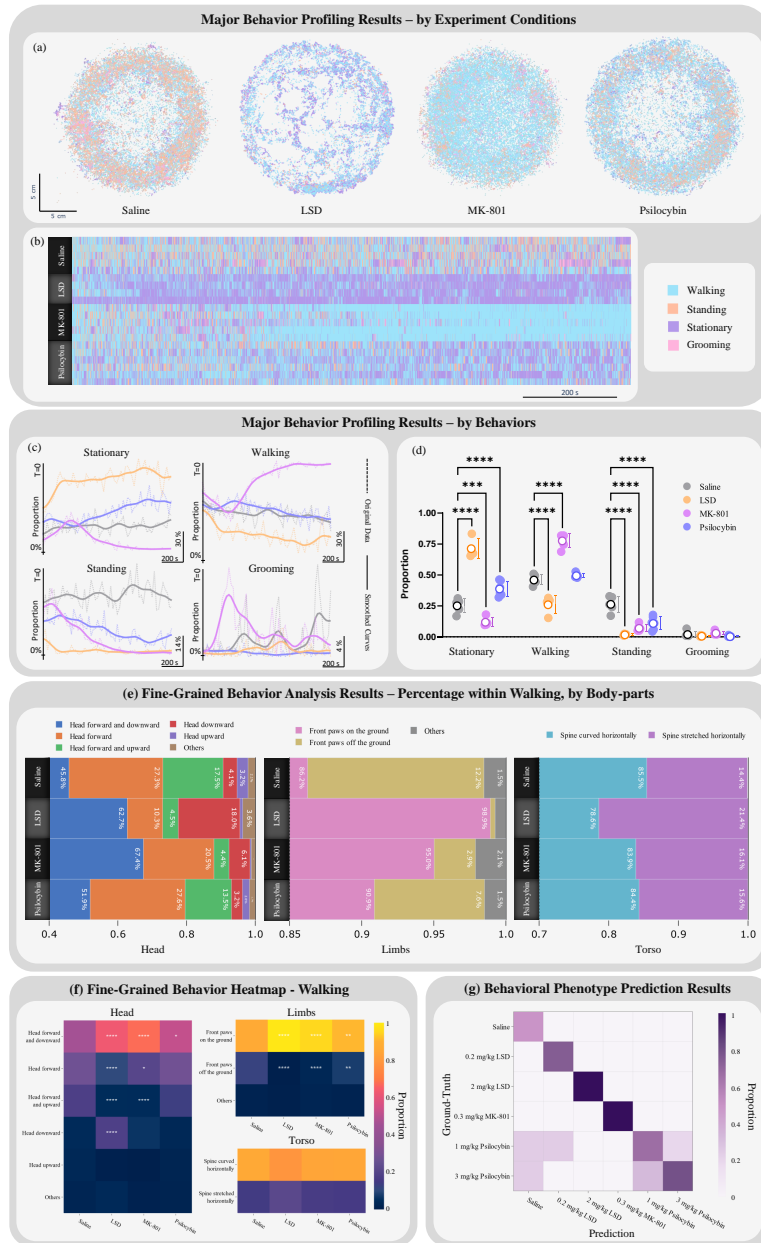


**Fig. 4 MouseGPT Analyzes Distinct Phenotypes of Spontaneous Behaviors Induced by Hallucinogens.** (a) Spatial Distribution of Major Behaviors: The spatial positions and behaviors of mice in a circular open field were mapped. Each circle represents all mice in a treatment group, with positions determined by spinal midpoints and behaviors color-coded as in (b). (b) Major Behavior Ethogram: Time-resolved behavior changes during the first 20 minutes post-treatment are depicted for each mouse in all groups, sampled consistently with (a). Rows represent individual mice, illustrating behavioral diversity. (c) Temporal Occurrence Patterns of Behaviors: Behavior proportions within 20-second time windows were visualized for different treatments. Dashed lines show group averages, and smoothed solid lines highlight trends, all starting from the same reference time T=0. Scales were adjusted to enhance the visualization of low-frequency behaviors. (d) Overall Behavioral Proportions: Mean behavior proportions during the entire recording session are presented with circles (mean) and error bars (95% confidence interval). Statistical significance was tested using two-way ANOVA with Tukey's multiple comparisons (\*\*p < 0.01; \*\*\*\*p < 0.0001). (e) Fine-Grained Postural Subtypes in Walking Behavior: Stacked bar charts illustrate the proportions of walking subtypes categorized by head, limb, and torso descriptors. Each bar represents the average subtype proportion across walking segments within each treatment group. (f) Heatmap of Fine-Grained Behaviors: Differences in fine-grained behavior proportions between drug-treated and control groups are visualized. Statistical significance was assessed using two-way ANOVA with Dunnett's multiple comparisons (\*p < 0.05; \*\*p < 0.01; \*\*\*\*p < 0.0001). (g) Drug Prediction Matrix: MouseGPT predicted drug treatments based on behavioral phenotypes, using data from six treatment groups (n=23). Columns indicate actual treatment groups, and color intensities reflect the proportion of mice assigned to each predicted group.



description generation, followed by embedding and clustering to obtain behavioral classification results for all mice (Extended Fig. 6a,b).

Based on these results, we mapped the spatial and temporal distribution of various behaviors in mice under different drug treatments (Fig. 4a,b), and quantified the occupancy (Fig. 4c,d). The results indicated that all hallucinogenic drugs induced changes in the occupancy of multiple behaviors and their occurrence patterns in the arena. These differences collectively suggest that LSD approximates a state of sedation in mice, Psi moderately reduces mouse activity, while MK801 induces a state of hyperactivity.

Subsequently, we further analyzed whether different drugs affected the internal structure of various behaviors, that is, whether the postures within each behavior category (defined by the geometric characteristics and relative positional relationships of body parts) differed in type and proportion. We selected walking, a behavior with diverse postures, and explored the distribution of different behavioral subtypes from the dimensions of the head, limbs, and torso (Fig. 4e and Extended Fig. 7). None of the drugs altered the internal categories of walking behavior, but they significantly affected the proportion and timing of specific posture types (Fig. 4f).

Finally, we utilized the built-in behavioral phenotype classifier of MouseGPT to test whether MouseGPT could accurately predict the relationships between different drugs. By integrating the existing behavioral results, the classifier was able to discriminate between known and unknown drugs with a high degree of accuracy (Fig. 4g).

Through the analyses presented above, we elucidated the specific differences in the phenotypic manifestations of hallucinatory behavior induced by three distinct drugs, thereby constructing individual behavioral profiles. These findings serve as significant assessment tools and indicators for further investigation into the neurobiological mechanisms underlying hallucination generation, as well as for evaluating drug-specific modification effects.

## 2.5 MouseGPT provides a user interface for natural language interaction

We have developed a LangChain-based [43] framework for mouse behavior analysis, enabling users to interact with an Agent through natural language. The framework incorporates the core analysis methods used in MouseGPT, such as clustering, fine-grained behavioral analysis, and statistical summarization, to address various user requirements.

At the heart of this framework is a robust Agent powered by a Large Language Model that processes open-ended natural language input. The Agent can analyze long video sequences holistically or examine specific frames in detail. Rather than processing raw data directly, the Agent leverages a range of tools to access the extensive MouseGPT database, enhancing efficiency and scalability (Fig. 5b).

The Agent’s toolset includes all of MouseGPT’s analytical methods—such as clustering, fine-grained behavior analysis, and novel behavior discovery—as well as tools integrated into the interactive UI. If the current tools fall short, the Python REPL

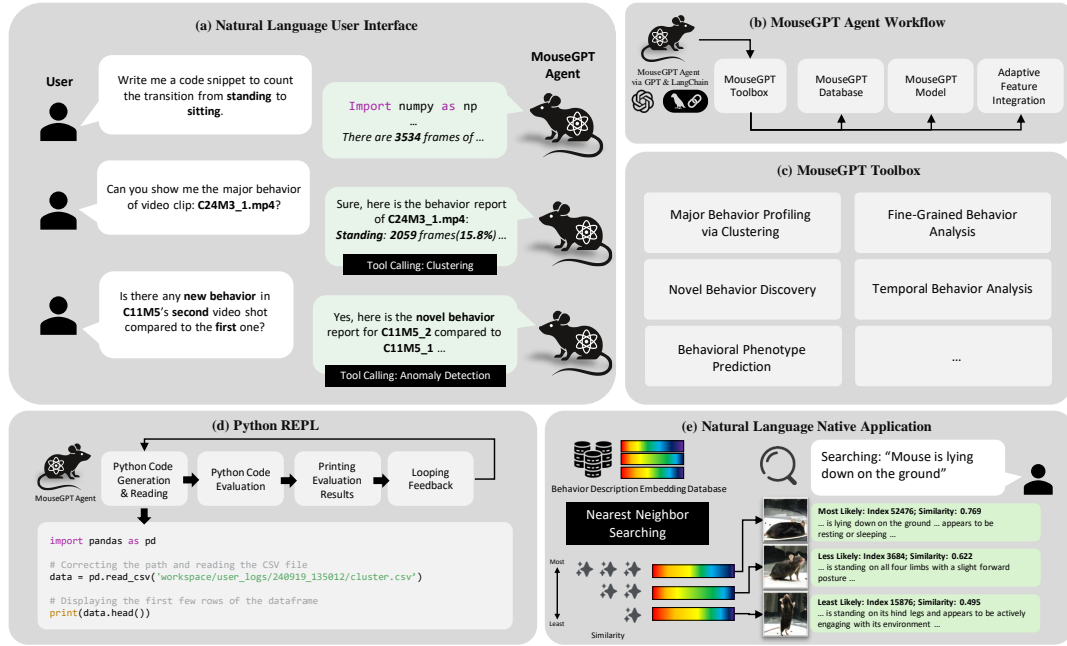


**Fig. 5 MouseGPT Natural Language User Interface.** (a) Interactive Interface: Users engage with the MouseGPT agent through natural language to perform clustering, behavior search, and automated code generation and execution, enabling intuitive interaction. (b) Agent Workflow: The agent integrates data access, MouseGPT model invocation, and analysis tasks via a unified workflow, streamlining complex behavior analyses. (c) Toolbox Overview: A comprehensive suite of tools supports major behavior profiling, fine-grained analysis, novel behavior detection, temporal analysis, and phenotype prediction. (d) Python REPL Integration: The agent dynamically generates and executes Python scripts to process data, exemplifying seamless automation. (e) Behavior Search: Embedding-based retrieval matches user-specified behaviors to the database, ranking results by similarity for precise behavior identification.

tool (Fig. 5d) enables the Agent to dynamically generate and execute code in a virtual environment, offering flexibility for custom tasks.

The search tool empowers users to query behaviors using natural language descriptions (e.g., “Mouse is lying down on the ground”). The tool maps input into high-dimensional features, retrieving the most relevant frames for detailed behavioral analysis (Fig. 5e). Throughout the process, the Agent summarizes the outputs from each tool as text, integrating them into the conversation to provide context for subsequent tasks (Fig. 5a).

### 3 Discussion

Developing an effective method to quantify mouse behavior and uncover the biological insights within their natural movement remains a significant challenge in computational ethology [44, 45]. In this study, we have, for the first time, used natural language as a powerful and flexible medium to describe mouse movement, serving as the key

feature for analyzing large-scale mouse behavioral data. Inspired by the explosive emergence of large-scale multi-modal models, we present MouseGPT, a foundation model for understanding mouse behavior. With Supervised-Fine-Tuning (SFT) on our datasets, MouseGPT is capable of automatically providing detailed and accurate descriptions of the behavioral states and body-part characteristics of mice in images. The advent of this model will enable researchers to obtain behavioral data to an unprecedented extent and will aid in the establishment of a standard database of animal behavior under various application cases including psychiatric disorders and drug discovery [46].

We have developed a comprehensive analysis framework that transforms MouseGPT’s outputs into analyzable insights for behavioral research. First, to ensure that the generated open-vocabulary descriptions are both informative and consistent across various conditions, we adopted a criterion that imitates the strategy used by humans when parsing behavior. This approach enables the model to produce hierarchical behavioral information, such as the activity state of mice (stationary or in-motion), the likely current behavior, and detailed posture descriptions. We then convert the textual descriptions into computable features, such as high-dimensional embeddings, which are processed through our analysis framework to perform tasks like major behavior profiling, fine-grained behavior analysis, novel behavior discovery, etc. We then showcased the effectiveness of these tools through a series of case studies in our work. By integrating these methods, MouseGPT reached ideal performance in two main challenges faced by kinematic-based unsupervised methods: accurate labeling and segmentation of various behaviors within continuous segments [20, 23], and comprehensive coverage and flexible selection of behavioral categories from coarse-to-fine granularity [21].

Furthermore, to provide a more intuitive interaction and seamless integration with large multi-modal models, we developed a natural language interface that transforms MouseGPT into an end-to-end behavioral analysis platform. Users can guide MouseGPT to perform specific behavioral analysis tasks through simple natural language commands, tailored to their research objectives. This flexibility and customizability enable MouseGPT to accommodate a variety of research needs.

Still, MouseGPT has certain limitations related to the performance ceiling of current visual-language models. Specifically, it can only analyze recorded videos as individual images, which may lead to the omission of certain behavioral details that occur over very short time spans, such as single instances of scratching or head twitching, as well as behaviors with special temporal patterns, like small-amplitude repetitive movements. In contrast, existing unsupervised methods are more sensitive to these subtle features [47, 48]. Therefore, we wish to emphasize that the semantic-based behavioral quantification method employed in MouseGPT is not in conflict with the mainstream kinematic data-based quantification methods, but rather, they are highly complementary. MouseGPT can integrate diverse kinematic data, such as the positional relationships or geometric information between specific limbs. This integration may occur through textual prompts before generating semantic results, allowing for more precise descriptions. Concurrently, MouseGPT’s cognitive abilities regarding the real world and its descriptive capabilities for open vocabulary can provide a reliable

and well-generalized classification framework for traditional unsupervised methods. Thus, we are confident that the combination of these two methods will further revolutionize our acquisition and understanding of behavioral data, promoting broader applications in the study of animal behavior.

For future development, we plan to apply MouseGPT to more scenarios, including drug discovery, social behavior studies, and behavior modeling and aim to collect extensive behavioral data to build a behavioral map of mice across different ages, times, drug treatments, and disease states, further enhancing MouseGPT’s recognition and prediction capabilities. Additionally, as the field of large-scale language and vision models continues to grow rapidly, with increasing capabilities and decreasing costs, we will continuously update MouseGPT to leverage new advancements, such as improved temporal modeling, better integration of multimodal data, and enhanced scalability. Our current modular design of the MouseGPT model and framework enables us to quickly iterate and conveniently integrate these new features. As a next step, we will develop MouseGPT’s Vision-Language Models for video understanding, aiming to incorporate more detailed temporal information to improve model inference and provide an end-to-end solution for animal ethology.

## References

- [1] John W. Krakauer, A. G.-M. M. A. M., Asif A. Ghazanfar & Poeppel, D. Neuroscience needs behavior: Correcting a reductionist bias. Neuron (2017).
- [2] Adam J. Calhoun, J. W. P. & Murthy, M. Unsupervised identification of the internal states that shape natural behavior. Nat Neurosci 22, 2040–2049 (2019).
- [3] Sandeep Robert Datta, K. B.-P. P., David J. Anderson & Leifer, A. Computational neuroethology: A call to action. Neuron **104**, 11–24 (2019).
- [4] Nestler, E. J. & Hyman, S. E. Animal models of neuropsychiatric disorders. Nature Neuroscience (2010).
- [5] Hiroshi Ueno, S. M. K. W.-Y. M. M. O., Yu Takahashi & Ishihara, T. Effect of simultaneous testing of two mice in the tail suspension test and forced swim test. Sci Rep (2022).
- [6] Slattery, D. A. & Cryan, J. F. Using the rat forced swim test to assess antidepressant-like activity in rodents. Nature Protocols (2012).
- [7] Anand Gururajan, J. F. C., Andreas Reif & Slattery, D. A. The future of rodent models in depression research. Nature Reviews Neuroscience (2019).
- [8] John F. Cryan, A. V., Cedric Mombereau. The tail suspension test as a model for assessing antidepressant activity: Review of pharmacological and genetic studies in mice. Neuroscience & Biobehavioral Reviews (2005).
- [9] Alex Gomez-Marin, A. R. K. R. M. C., Joseph J Paton & Mainen, Z. F. Big behavioral data: psychology, ethology and the foundations of neuroscience. Nature Neuroscience (2014).
- [10] Lindsay P. Cameron, J. L. A. J. P. Z. Q. H. Y. E. M. V. V. M. N. M. J. C. T. D. M.-T. T. L. B. Y. L. J. L. E. I. A. G. Z. J. V. B. M. B. M. T. L. E. D. Z. T. R. O. F. H. W. J. D. M. P. J. L. D. K. D. R. J. P. Y. Z., Robert J. Tombari & Olson, D. E. A non-hallucinogenic psychedelic analogue with therapeutic potential. nature (2021).
- [11] Linda Nocchi, M. D. R. D. M. M. A. T. L. C. E. P. C. H. C., Nainika Roy & Heppenstall, P. A. Interleukin-31-mediated photoablation of pruritogenic epidermal neurons reduces itch-associated behaviours in mice. Nature Biomedical Engineering (2019).
- [12] K. Schmack, T. O. J. F. S., M. Bosc & Kepecs, A. Striatal dopamine mediates hallucination-like perception in mice. Science (2021).
- [13] Fabrice de Chaumont, N. T. T. L. S. D. A. I. T. L. A.-M. L. S. P. F. T. B., Elodie Ey & Olivo-Marin, J.-C. Real-time analysis of the

- behaviour of groups of mice via a depth-sensing camera and machine learning. Nature Biomedical Engineering (2019).
- [14] Miwa Morita-Nakagawa, K. N. Y. I. S. S. W.-Z. G. M. F., Kohji Okamura & Li, X.-K. Supervised machine learning of outbred mouse genotypes to predict hepatic immunological tolerance of individuals. Scientific Reports (2024).
- [15] Luis A. Bolaños, N. L. F. J. M. L. P. K. G. C. D.-H. H. H. R., Dongsheng Xiao & Murphy, T. H. A three-dimensional virtual mouse generates synthetic training data for behavioral analysis. Nature Methods (2021).
- [16] Yaning Han, Y. W. W. L. Z. W. X. W. C. H. J. L.-K. H. S. C. Y. H. N. W. J. L. Y. S. J. L. G.-D. W. L. W. Y. Z., Ke Chen & Wei, P. Multi-animal 3d social pose estimation, identification and behaviour embedding with a few-shot learning framework. Nat Mach Intell 6, 48–61 (2024).
- [17] Tanmay Nath, A. C. C. A. P. M. B., Alexander Mathis & Mathis, M. W. Using deeplabcut for 3d markerless pose estimation across species and behaviors. Nat Protoc 14, 2152–2176 (2019).
- [18] Jessy Lauer, S. Y. W. M. S. S. T. N. M. M. R. V. D. S. D. S. G. F. V. N. M. G. L. C. D. M. W. M., Mu Zhou & Mathis, A. Multi-animal pose estimation, identification and tracking with deeplabcut. Nat Methods 19, 496–504 (2022).
- [19] Jens F. Tillmann, M. K. S., Alexander I. Hsu & Yttri, E. A. A-soid, an active-learning platform for expert-guided, data-efficient discovery of behavior. Nat Methods 21, 703–711 (2024).
- [20] Hsu, A. I. & Yttri, E. A. B-soid, an open-source unsupervised algorithm for identification and fast prediction of behaviors. Nat Commun 12, 5188 (2021).
- [21] Kang Huang, K. C. H. P. G. Z. W. Y. X. L. S. L. P. W., Yaning Han & Wang, L. A hierarchical 3d-motion learning framework for animal spontaneous behavior mapping. Nat Commun 12, 2784 (2021).
- [22] Kabra, M., Robie, A. A., Rivera-Alba, M., Branson, S. & Branson, K. Jaaba: interactive machine learning for automatic annotation of animal behavior. Nature methods 10, 64–67 (2013).
- [23] Kevin Luxem, F. F. J. K. S. R. M. J. J. P. S. R., Petra Mocellin & Bauer, P. Identifying behavioral structure from deep variational embeddings of animal motion. Commun Biol 5, 1267 (2022).
- [24] Talmo D. Pereira, L. W. M. K. S. S.-H. W. M. M., Diego E. Aldarondo & Shaevitz, J. W. Fast animal pose estimation using deep neural networks. Nat Methods 16, 117–125 (2019).

- [25] Timothy W. Dunn, K. S. S. D. E. A.-D. G. C. H. S. N. C. W. L. W. A. J. G. D. E. C. D. A. W. A. F. F. W., Jesse D. Marshall & Ölveczky, B. P. Geometric deep learning enables 3d kinematic profiling across species and environments. Nat Methods 18, 564–573 (2021).
- [26] Caleb Weinreb, S. L. M. A. M. O. L. Z. S. A. E. C. R. H. S. M. W. F. G. M. J. S. Y. A. M. M. W. M. T. P. S. W. L., Jonah E. Pearl & Datta, S. R. Keypoint-moseq: parsing behavior by linking point tracking to pose dynamics. Nat Methods 21, 1329–1339 (2024).
- [27] Adam Gosztolai, V. L.-R. M. P. A. D. M. H. R. P. F., Semih Günel & Ramdya, P. Liftpose3d, a deep learning-based approach for transforming two-dimensional to three-dimensional poses in laboratory animals. Nat Methods 18, 975–981 (2021).
- [28] Alexander B. Wiltschko, A. Z. R. A. W. F. G. J. E. M. R. E. P. J. K. M. J. J., Tatsuya Tsukahara & Datta, S. R. Revealing the structure of pharmacobehavioral space through motion sequencing. Nat Neurosci 23, 1433–1443 (2020).
- [29] Talmo D. Pereira, J. W. S. & Murthy, M. Quantifying behavior to understand the brain. Nat Neurosci 23, 1537–1549 (2020).
- [30] Talmo D. Pereira, A. M. D. M. T. J. L. S. R. E. S. P. E. N. D. S. D. Z. Y. W. G. C. M.-S. C. C. M. M. D. C. J. D. M. K. D. H. S. S. D. K. S. S.-H. W. A. L. F. J. W. S., Nathaniel Tabris & Murthy, M. Slep: A deep learning system for multi-animal pose tracking. Nat Methods 19, 486–495 (2022).
- [31] Matthew Christensen, N. Y., Milos Vukadinovic & Ouyang, D. Vision–language foundation model for echocardiogram interpretation. Nat Med 30, 1481–1488 (2024).
- [32] Haotian Cui, H. M. K. P. F. L. N. D., Chloe Wang & Wang, B. scgpt: toward building a foundation model for single-cell multi-omics using generative ai. Nat Methods 21, 1470–1480 (2024).
- [33] Di Peng, D. L. C. H. X. W. Y. Y. L. S. M. Z. Y. W. J. L. X. Y. Y. W. Z. F. X. H.-M. C. Y. G. Y. X., Liubin Zheng & Zhang, L. Large-language models facilitate discovery of the molecular signatures regulating sleep and activity. Nat Commun 15, 3685 (2024).
- [34] Chu, Y. et al. A 5' utr language model for decoding untranslated regions of mrna and function predictions. Nature Machine Intelligence 6, 449–460 (2024).
- [35] Lu, M. Y. et al. A multimodal generative ai copilot for human pathology. Nature 1–3 (2024).
- [36] Shen, J. et al. Unbiased organism-agnostic and highly sensitive signal peptide predictor with deep protein language model. Nature Computational Science 4,

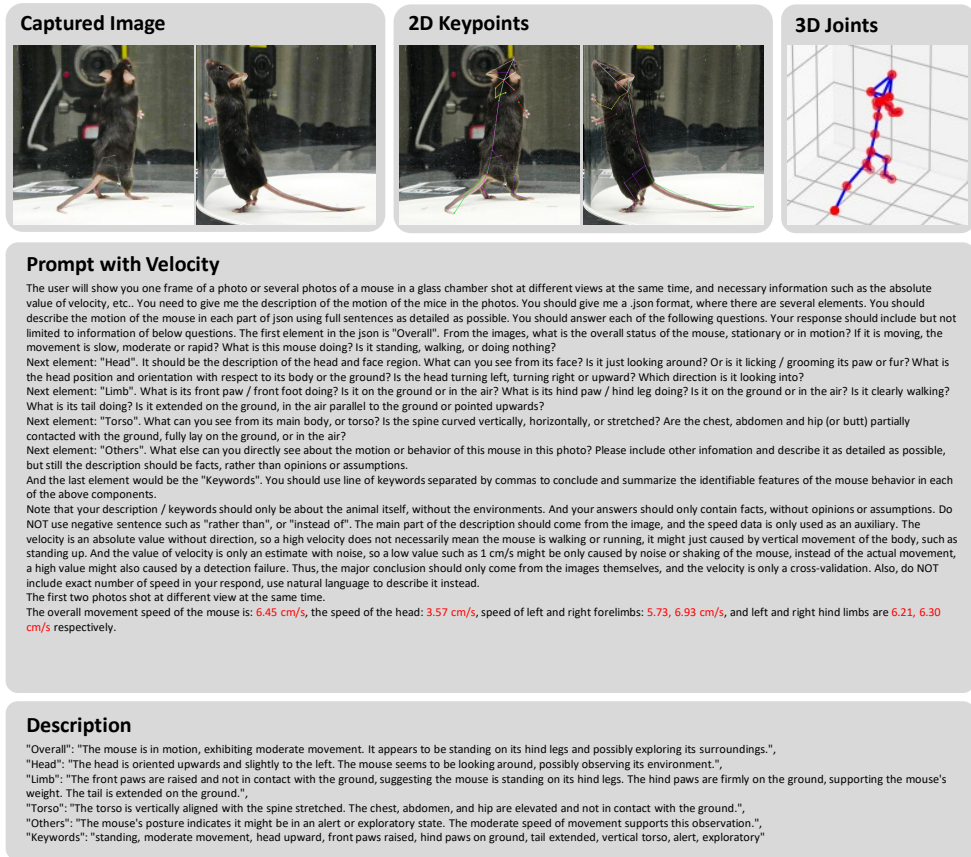


29–42 (2024).

- [37] Ye, S., Lauer, J., Zhou, M., Mathis, A. & Mathis, M. W. Amadeusgpt: a natural language interface for interactive animal behavioral analysis. Thirty-seventh Conference on Neural Information Processing Systems (2023). URL <https://openreview.net/forum?id=9AcG3Tsyoq>.
- [38] Chen, Z. et al. Internvl: Scaling up vision foundation models and aligning for generic visual-linguistic tasks. arXiv preprint arXiv:2312.14238 (2023).
- [39] Yao, Y. et al. Minicpm-v: A gpt-4v level mllm on your phone. arXiv preprint arXiv:2408.01800 (2024).
- [40] OpenAI. Text embedding model api. <https://platform.openai.com/docs/models/embeddings> (2024). Accessed: 2024-10-22.
- [41] McInnes, L., Healy, J. & Melville, J. Umap: Uniform manifold approximation and projection for dimension reduction. arXiv preprint arXiv:1802.03426 (2018).
- [42] OpenAI. Hello gpt-4o. <https://openai.com/index/hello-gpt-4o/> (2024). Accessed: 2024-10-22.
- [43] Chase, H. Langchain (2022). URL <https://github.com/langchain-ai/langchain>.
- [44] Anderson, D. & Perona, P. Toward a Science of Computational Ethology. Neuron **84**, 18–31 (2014). URL <https://linkinghub.elsevier.com/retrieve/pii/S0896627314007934>. Rate: 5 TLDR: This work explores the opportunities and long-term directions of research in the new field of Computational Ethology, made possible by advances in technology, mathematics, and engineering that allow scientists to automate the measurement and the analysis of animal behavior.
- [45] Pereira, T. D., Shaevitz, J. W. & Murthy, M. Quantifying behavior to understand the brain. Nature Neuroscience **23**, 1537–1549 (2020). URL <http://dx.doi.org/10.1038/s41593-020-00734-z>. Publisher: Springer Science and Business Media LLC rate: 5 TLDR: An overview of the latest advances in motion tracking and behavior prediction is provided and how quantitative descriptions of behavior can be leveraged to connect brain activity with animal movements, with the ultimate goal of resolving the relationship between neural circuits, cognitive processes and behavior.
- [46] Cao, D. et al. Structure-based discovery of nonhallucinogenic psychedelic analogs. Science **375**, 403–411 (2022). URL <https://www.science.org/doi/10.1126/science.abl8615>. Rate: 0 TLDR: Structures of the human serotonin 2A receptor show a second binding mode that might be leveraged to design non-hallucinogenic drugs, and arrestin-biased ligands that displayed antidepressant-like activity in mice without hallucination effects are designed.

- [47] Wiltchko, A., Johnson, M., Iurilli, G. & Peterson, R. Mapping Sub-Second Structure in Mouse Behavior. *Neuron* **88**, 1121–1135 (2015). URL <https://linkinghub.elsevier.com/retrieve/pii/S0896627315010375>. Rate: 4 TLDR: Depth imaging is used to show that 3D mouse pose dynamics are structured at the sub-second timescale and reveals that mouse body language is built from identifiable components and is organized in a predictable fashion; deciphering this language establishes an objective framework for characterizing the influence of environmental cues, genes and neural activity on behavior.
- [48] Weinreb, C. et al. Keypoint-MoSeq: parsing behavior by linking point tracking to pose dynamics. *Nature Methods* **21**, 1329–1339 (2024). URL <https://www.nature.com/articles/s41592-024-02318-2>. Rate: 5 TLDR: Keypoint-MoSeq renders accessible the modular structure of behavior through standard video recordings, and outperforms commonly used alternative clustering methods at identifying transitions, at capturing correlations between neural activity and behavior and at classifying either solitary or social behaviors in accordance with human annotations.
- [49] Contributors, M. MMYOLO: OpenMMLab YOLO series toolbox and benchmark. <https://github.com/open-mmlab/mmyolo> (2022).
- [50] Contributors, M. Openmmlab pose estimation toolbox and benchmark. <https://github.com/open-mmlab/mmpose> (2020).
- [51] Jocher, G. et al. ultralytics/yolov5: v7.0 - YOLOv5 SOTA Realtime Instance Segmentation (2022). URL <https://doi.org/10.5281/zenodo.7347926>.
- [52] Wang, J. et al. Deep high-resolution representation learning for visual recognition (2020). URL <https://arxiv.org/abs/1908.07919>. 1908.07919.
- [53] Easymocap - make human motion capture easier. Github (2021). URL <https://github.com/zju3dv/EasyMocap>.
- [54] Chen, Z. et al. How far are we to gpt-4v? closing the gap to commercial multimodal models with open-source suites. *arXiv preprint arXiv:2404.16821* (2024).
- [55] Vaswani, A. Attention is all you need. *Advances in Neural Information Processing Systems* (2017).
- [56] Dubey, A. et al. The llama 3 herd of models. *arXiv preprint arXiv:2407.21783* (2024).
- [57] Yang, A. et al. Qwen2 technical report. *arXiv preprint arXiv:2407.10671* (2024).
- [58] Zhai, X., Mustafa, B., Kolesnikov, A. & Beyer, L. Sigmoid loss for language image pre-training, 11975–11986 (2023).

- [59] Aminabadi, R. Y. et al. Deepspeed-inference: enabling efficient inference of transformer models at unprecedented 1–15 (IEEE, 2022).
- [60] OpenAI. New embedding models and api updates (2024). URL <https://openai.com/index/new-embedding-models-and-api-updates/>. Accessed: 2024-12-05.
- [61] Abid, A. et al. Gradio: Hassle-free sharing and testing of ml models in the wild. arXiv preprint arXiv:1906.02569 (2019).



**Extended Fig. 1 Data Sample from the MouseGPT Dataset.** An example of a single data sample from the MouseGPT Dataset, illustrating how multi-view images, 3D joint keypoints, and velocity data are combined to produce structured, open-vocabulary behavioral descriptions. The figure demonstrates the dataset's ability to capture detailed annotations for overall behavior, head orientation, limb positioning, torso posture, and additional traits, summarized through concise keywords.

## 4 Methods

### 4.1 Data Collection and Experiment Settings

#### *Dataset Overview*

We collected and curated a comprehensive open-vocabulary dataset to train and evaluate MouseGPT, our model for understanding mouse behavior. This dataset encompasses synchronized multi-view video sequences, 3D keypoint annotations for each frame (see Data Annotation and Curation), detailed textual descriptions (see Automated Open-vocabulary Behavior Annotation), as well as metadata related to medication and mouse modeling (see Animals and Husbandry).

Using a multi-view acquisition system, we finally gathered 75 multi-view videos of 55 different mice, totaling over 1,486 minutes and 42,822,048 frames across 5,352,756 time points. Each frame was automatically annotated with 3D keypoints and 2D bounding boxes to capture the precise position and movement of the mice. After training our models, 892,131 frames from experimental scenarios were automatically annotated with detailed open-vocabulary descriptions using our MouseGPT models, MouseGPT-Large, and MouseGPT-Lite. We plan to make this dataset publicly available to benefit the research community (see Data Availability).

We also developed two dedicated datasets for model training. The first dataset, used to train our 3D keypoint detection system, contained 2,161,416 manually labeled keypoints across 90,059 images. The second dataset was created for training the Vision-Language Model (VLM), where GPT-4o was utilized to generate detailed textual descriptions for 45 video sequences involving 37 mice, followed by a data curation process that produced 270,085 high-quality frame-level open-vocabulary annotations.

### ***Animals and Husbandry***

A total of 55 8-12-week-old C57BL/6J male mice (Silaike Experiment Animal Co., Ltd., JAX:000664) were used for recording and analysis in this study, including 24 mice for depression behavior capture and 31 mice for hallucination. After introduced into the colony at 8 weeks, mice were housed in groups of 4 to 5 per cage to habituate for at least 1 week with a controlled temperature of 22-25°C, and 40-70% humidity. Food and water were provided ad libitum. The circadian rhythm of the mice varied according to the different experiments. For mice in depression experiments, they were kept under a normal 12-hour light-dark cycle (lights on from 7:00 am to 7:00 pm). In contrast, mice in the hallucination experiments were placed under the reverse 12-hour cycle. All experiments procedures were approved by the Institutional Animal Care and Use Committee (IACUC) of ShanghaiTech University.

### ***Behavioral experiment***

In depression behavior experiment, we randomly select  $n=16$  mice as Chronic Restraint Stress (CRS) group and  $n=8$  as control group. CRS mice were put into 50 mL conical tubes during the light phase for 2–3 h per day for 16 consecutive days. Holes were drilled on the tubes to enable mice to breathe freely. We recorded the mice on the day following the end of restraint, and then assessed their level of depression using the Tail Suspension Test (TST), in which mice were suspended by binding their tail with adhesive tape fastened to a rail 50 cm from the ground. A 6-minute video recording started immediately after the mice were taped. The immobility duration in the last 4 minutes of the experiment was measured by another member of our group who was blinded to mouse treatment. Finally, Mice with immobility duration higher than the average time of the control group were classified as depression-like mice. To avoid the potential cumulative effects of hallucinogenic drugs, all mice in this experiment were recorded only once after drug administration to ensure the reliability of subsequent analysis.

### ***Drug treatment***

We selected two classic hallucinogens, Lysergic acid diethylamide (LSD) and Psilocybin (both from Laboratory of Medicinal Chemistry and Biology, Changchun Institute of Applied Chemistry, Chinese Academy of Sciences), as well as MK801 (ApexBio, Cat#A3100), an NMDA receptor antagonist, to induce hallucination-related behaviors in mice. Psilocybin and LSD in powder form were initially dissolved in 0.9% saline to a concentration of 1 mg/mL, then stored in a  $-80^{\circ}\text{C}$  freezer until the day of use, when they were further diluted with fresh 0.9% saline. MK801 was first dissolved in DMSO and then diluted with 0.9% saline on the day of use. All drugs were delivered via intraperitoneal injection. During the two days prior to behavior recording, the mice, in their home cages, were transferred to the recording facility for 1-2 hours to preliminarily acclimate to the environment, typically during the same time window as the recording sessions (1:00 pm to 3:00 pm).

### ***Video Recordings***

In our data collection settings (Fig. 2a-left), all 55 mice that appeared in our dataset were captured under the same controlled conditions and using identical capture devices. The capture setup consists of 8 synchronized Z-Cam E2 cinema cameras with Olympus 14-42mm 1:3.5-5.6 EZ lenses, capturing at 4K resolution, 60 FPS. The cameras are connected in a daisy-chain configuration, with the first camera serving as the master camera to send synchronization signals, and the remaining seven cameras functioning as slave cameras to ensure synchronization. Seven cameras are arranged centrally on a circular ring with a diameter of 1.5 meters at the same height as the mouse activity surface, directed towards the center of the activity area. Additionally, one camera is mounted at the top of the apparatus at a height of 1.2 meters, capturing footage from above with the center of the mouse activity area as the focal point.

On the day of recording, the mice were transferred to the recording facility 1 hour in advance and kept under dark conditions. Video recording began immediately after the mice were moved from their home cages to an open arena with a diameter of 25 cm, and continued for 20 minutes. The arena was then cleaned and prepared for the next mouse.

### ***Camera Calibration***

In order to acquire accurate 3D information from 2D camera arrays, we pre-calibrate our camera using Agisoft Metashape 2.0.2. The camera calibration process includes camera intrinsic calibration and extrinsic calibration. During the camera intrinsic calibration process, we used a MacBook Pro (15-inch, 2017) to display a  $22 \times 14$  checkerboard pattern, ensuring that the pattern was presented on a perfectly flat surface. With all cameras set to the same recording parameters as those used in the actual sessions, the checkerboard pattern was shown to each camera from various positions and angles, covering the entire capture area. The Agisoft Metashape 2.0.2 is used to calculate the camera intrinsic parameters, including the focal length:  $f$ , principal point coordinates:  $c_x$ ,  $c_y$ , radial distortion coefficients:  $k_1$ ,  $k_2$ ,  $k_3$ , and the tangential distortion coefficients:  $p_1$ ,  $p_2$ . These parameters are calculated from observation of chessboard, used for correcting lens distortions and ensuring accurate image capture.

Once calibrated, these parameters are preserved the same during all of the dataset recording sessions.

The camera extrinsic calibration process was conducted differently to account for potential movements of the recording apparatus during filming, as well as shifts caused by gravity. To ensure accuracy, the extrinsic calibration was performed each day before the recording sessions, and the calibration results were only valid for the recordings made on that particular day. We printed an auxiliary pattern for extrinsic calibration on an A3-sized sheet of paper (with dimensions of  $297 \times 420$ -mm). The central area of the calibration sheet was left blank, measuring  $250 \times 250$ -mm, to preserve the mouse activity area. At the center of this blank area, a black dot with a diameter of 3mm was printed to serve as the origin of the coordinate system. Alignment patterns, each consisting of two AR Tags, were printed in the four corners of the calibration sheet. The distance between the centers of each pair of alignment patterns was 26.0 cm along the long side and 24.0 cm along the short side. This information was used in the subsequent calibration calculations. The calibration sheet was carefully adhered to the base of the recording apparatus to ensure the accuracy of the calibration pattern.

We designed calibration objects with complex pattern features that cover a  $25.0 \times 25.0$ -cm area. These objects included various cubes and rectangular prisms, which were placed within the filming area. Using the 48mm lens of an iPhone 15 Pro Max (which had also undergone the intrinsic calibration process described earlier), we captured 20-50 photos uniformly sampled between each pair of adjacent cameras among the eight cameras. The purpose of this uniform sampling was to supplement the eight sparsely distributed cameras with sufficiently dense observational angles, allowing for a more accurate determination of the spatial positions of the primary cameras.

The sampled photos, along with images from the eight main cameras, were then imported into MetaShape for extrinsic camera calibration. During this process, we manually marked the five previously mentioned markers (the center point of the activity area and the center points of the four corner calibration patterns) within the viewpoints of the eight main cameras. These markers were assigned their actual distances in the reference module, establishing a 3D right-handed coordinate system with the activity area center as the origin.

Next, we manually selected 5%-10% of the iPhone-captured images and similarly annotated the five markers. Using MetaShape’s extrinsic calibration tools, we aligned the photos with a Key Point Limit of 15,000 per Mpx, a Tie Point Limit of 10,000, and enabled features such as Guided Image Matching, Adaptive Camera Model Fitting, and Highest Accuracy. After aligning the photos, we performed an “Optimize Camera Alignment” process to further refine the 3D positions and rotations of the cameras.

With this, we completed the intrinsic and extrinsic camera calibration process. The resulting camera parameter files will be used for 3D spatial computations, supporting tasks such as pose estimation and speed calculation.

## 4.2 Data Annotation and Curation

### *Overview: Data Annotation and Curation*

We developed a comprehensive data annotation and curation workflow for training and evaluating the MouseGPT model, using a combination of manual and automated



Hi, please help me analyze this data by clustering it.

```
{'static': {'crouched': 0.050175029171528586, 'standing': 0.012835472578763127, 'walking': 0.4027337889648275, 'grooming': 0.018503083847307884}, 'save_path': 'workspace/user_logs/241101_173245_fe7e2300370d4a4daf3daefcaa22e58a/cluster.csv/result.csv'}
```

The clustering analysis of the mouse behavior data has been completed. Here are the statistics of the clustering results:

- Crouched: 5.02%
- Standing: 1.28%
- Walking: 40.27%
- Grooming: 1.85%

The results have been saved to the following path: `workspace/user\_logs/241101\_173245\_fe7e2300370d4a4daf3daefcaa22e58a/cluster.csv/result.csv`.

Can you help me find some frames of "mice using two-legged standing"?

```
{'top_5': ['00014148', '00000336', '00060816', '00056844', '00009360'], 'save_path': 'workspace/user_logs/241101_173245_fe7e2300370d4a4daf3daefcaa22e58a/search_mice_using_two-legged_standing.csv/result.csv'}
```

I found the frames where the behavior "mice using two-legged standing" is observed. Here are the top 5 frame indices:

1. 14148
2. 336
3. 60816
4. 56844
5. 9360

The results have been saved to the following path: `workspace/user\_logs/241101\_173245\_fe7e2300370d4a4daf3daefcaa22e58a/search\_mice\_using\_two-legged\_standing.csv/result.csv`.

Can you help me write some code to find the number of times the mouse "switched from standing to walking"?

```
import pandas as pd

data = pd.read_csv('workspace/user_logs/241101_173245_fe7e2300370d4a4daf3daefcaa22e58a/cluster.csv/result.csv')

# Display the first few rows to understand the structure
print(data.head())
```

```
NotADirectoryError(20, 'Not a directory')
```

```
# Load the clustering result CSV file directly
file_path = 'workspace/user_logs/241101_173245_fe7e2300370d4a4daf3daefcaa22e58a/cluster.csv'
data = pd.read_csv(file_path, sep=',')

# Display the first few rows to understand the structure
print(data.head())
```

The columns have been correctly identified as 'frame\_id' and 'behavior'. Now, let's proceed to count the number of times the mouse switches from "standing" to "walking"

```
# Count the number of times the mouse switches from 'standing' to 'walking'

# Initialize a counter
switch_count = 0

# Iterate through the data to count the transitions
for i in range(1, len(data)):
    if data.iloc[i-1]['behavior'] == 'standing' and data.iloc[i]['behavior'] == 'walking':
        switch_count += 1

print(switch_count)
```

The mouse switched from "standing" to "walking" a total of 342 times in the dataset.

User Input

Tool Call

Agent Output

**Extended Fig. 2 Dialogue Sample Between User and MouseGPT Agents.** An example of a natural language interaction showcasing the capabilities of the MouseGPT Agent. The dialogue demonstrates user queries for behavior-specific frame retrieval, clustering analysis, and code generation for analyzing behavioral transitions. The agent effectively combines tool invocation, data processing, and execution to deliver actionable results, illustrating its versatility and ease of use for mouse behavior analysis tasks.

methods to create a robust dataset. This workflow generated pose estimates and 2D/3D kinematic data, providing essential spatial and temporal information for VLM inference. Subsequently, we applied an automatic annotation strategy using the VLM to generate open-vocabulary behavioral descriptions (Extended Fig. 1).

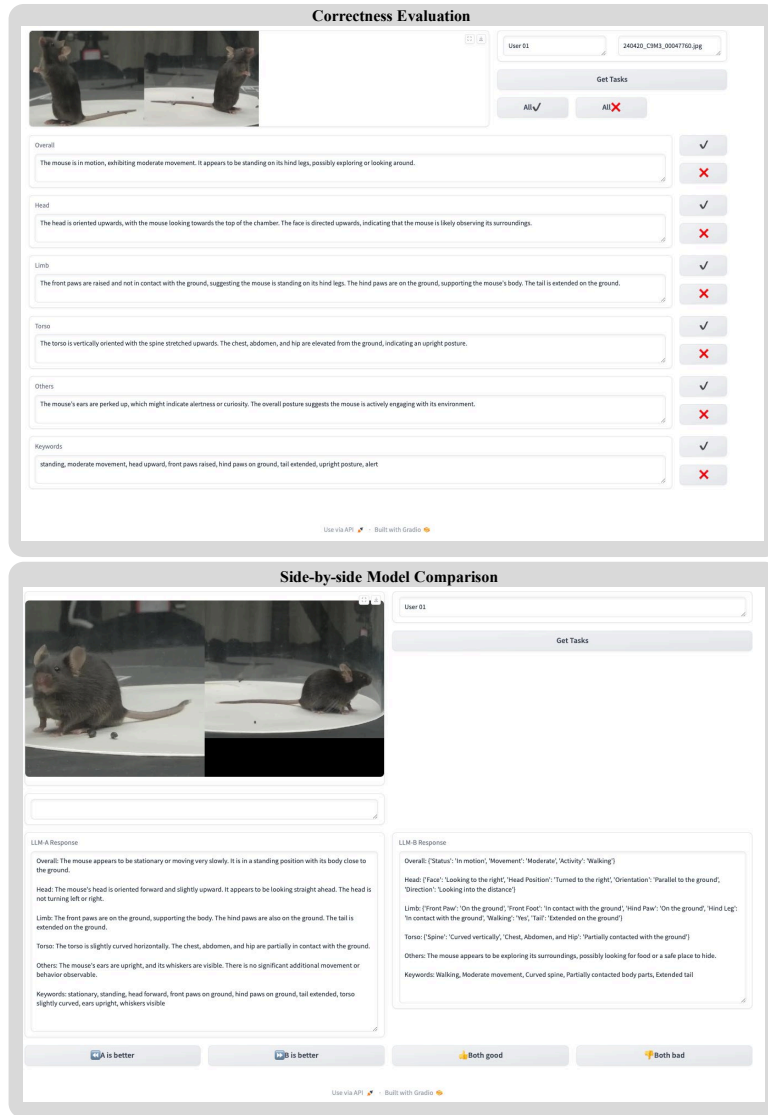
Our approach began with manual annotation of 2D poses from eight different perspectives. Specifically, we annotated 2,161,416 keypoints across 90,059 images, providing a high-quality labeled dataset that served as the foundation to train a neural network for automated kinematic data extraction across the MouseGPT dataset. Automated pose estimation was conducted using well-established models, such as YOLOv5 and HRNet-based architectures. Through these methods, we obtained accurate 2D and 3D poses, and thus calculated velocities, which served as input to Vision-Language Models (VLMs), providing essential spatial and temporal information for understanding complex mouse behaviors across different experimental conditions.

With the essential spatial and temporal data in place, we used an automatic annotation strategy for generating open-vocabulary behavioral descriptions, enabling a broader contextual understanding of mouse activity that can be directly queried using natural language. Through this automated yet flexible pipeline, we efficiently extracted and labeled kinematic and descriptive data, creating a comprehensive resource for downstream behavioral analysis and supporting novel insights into ethological research.

### *Data Pre-processing and Augmentation*

Index	Label	Detailed Description
1	EarL	Tip of the Left Ear
2	EarR	Tip of the Right Ear
3	Snout	Tip of the Snout
4	SpineF	Beginning of the Spine
5	SpineG	First Tripartite Point of the Spine
6	SpineH	Second Tripartite Point of the Spine
7	Hip	Hip Joint
8	Tail (base)	Base of the Tail
9	Tail (mid)	Middle Section of the Tail
10	Tail (end)	Tip of the Tail
11	ForepawL	Tip of the Left Forepaw
12	WristL	Left Wrist Joint
13	ElbowL	Left Elbow Joint
14	ShoulderL	Left Shoulder Joint
15	ForepawR	Tip of the Right Forepaw
16	WristR	Right Wrist Joint
17	ElbowR	Right Elbow Joint
18	ShoulderR	Right Shoulder Joint
19	HindpawL	Tip of the Left Hindpaw
20	AnkleL	Left Ankle Joint
21	KneeL	Left Knee Joint
22	HindpawR	Tip of the Right Hindpaw
23	AnkleR	Right Ankle Joint
24	KneeR	Right Knee Joint

**Table 1** Body Part Labels and Descriptions



**Extended Fig. 3 Expert Evaluation User Interface.** An interface designed for expert evaluation of MouseGPT’s performance. The interface allows experts to assess the correctness of model-generated behavior descriptions and conduct pairwise comparisons between MouseGPT and other models.

In this study, meticulous data preprocessing and augmentation procedures were employed to ensure the robustness and accuracy of our annotated datasets. We utilized a MATLAB-based software, Label3D, to perform precise 3D annotations from multiple 2D views captured simultaneously from eight distinct angles. We defined our own keypoint configuration, comprising 24 keypoints (Table 1) aligned with essential

skeletal landmarks on the mouse—such as the snout, various spine segments, limbs, and tail—based on insights from established works like DANNCE and SLEAP.

The anatomical keypoints were meticulously defined to capture motions of the mouse in three-dimensional space, with 24 distinct skeletal landmarks representing critical joints and body segments integral to movement analysis. These included keypoints like EarL and EarR for orientation, Snout for head position, and SpineF, SpineG, and SpineH for spinal movements. Notably, SpineG and SpineH are located as two equidistant points between SpineF and Hip, further enhancing the granularity of spinal movement analysis. Additionally, various points along the limbs and tail were annotated for detailed movement studies.

The annotation process commenced by marking each keypoint in at least two camera views, followed by employing the “triangulate” function to project these 2D points into 3D space. This initial automated triangulation provided a baseline, which was refined through manual adjustments of the 2D annotations and subsequent re-triangulation, thus enhancing the accuracy. This iterative process ensured the consistent placement of keypoints across all views.

For keypoints obscured by complex mouse movements or overlapping anatomical features, an additional validation step was implemented to enhance precision. Each annotation was rigorously reviewed, and those identified as being of poor quality are re-annotated. This meticulous validation process helps mitigate errors stemming from both the automated triangulation inaccuracies and subjective judgments during manual annotation, thus bolstering the reliability and consistency of the dataset for subsequent analytical tasks.

To facilitate the effective localization of mice within images, our initial step involved the generation of bounding boxes. We computed the minimum bounding box enclosing all detected keypoints on the mice. To accommodate any variations in the mice’s positioning and ensure the entire object was captured, we added a 35-pixel padding to each side of the bounding box. This precaution prevents the bounding boxes from being overly restrictive, thereby enhancing the robustness of the subsequent detection and analysis tasks.

In preparation for the use of the YOLOv5 model, it was imperative to optimize anchor points, which serve as preliminary candidate bounding boxes for object prediction. Given that objects in different datasets exhibit diverse sizes and aspect ratios, unsuitable anchors could impair the model’s ability to precisely localize objects. To address this, we conducted an analysis of the bounding boxes of the target object using K-Means clustering. This analysis aimed to optimize the anchor sizes and aspect ratios, thereby enabling dynamic adjustments during training to better align with the object distribution in our dataset. This alignment is crucial for enhancing the detection accuracy and the generalization capabilities of the model.

Data augmentation is essential in enhancing the model’s adaptability and performance during the preprocessing phase. To optimize the input for the mmyolo [49] and mmpose [50] networks, we adjusted the size of the images, which not only conforms to the network requirements but also facilitates faster processing. Focusing on strengthening the model’s ability to generalize across diverse scenarios and increase its resilience to overfitting, we implemented a variety of data augmentation strategies. Specifically,

we applied random cropping to simulate different object positions and scales, horizontal flipping to introduce variability in object orientation, random rotation to account for various object angles, and color jittering to ensure robustness against variations in lighting and color. These augmentation techniques diversify the training dataset, promoting the development of more universal feature recognition within the model and minimizing its tendency to overfit specific patterns. This strategic enhancement of data variability ensures that our model maintains high performance under a wide range of environmental conditions and animal movements.

### *2D Kinematics Estimation Workflow and Network Design*

In order to automatically estimate 2D kinematic information from video sequences, we employed a two-stage detection and pose estimation framework, utilizing the mmyolo and mmpose training frameworks provided by mmlab to ensure better processing speed and robustness.

In the first stage, we use the YOLOv5-s [51] network as the object detector to detect and extract the bounding boxes of mice from the input images. YOLOv5 is a widely-used real-time object detection network that offers a good balance between speed and accuracy. The network consists of three main components: the backbone, neck, and head. The backbone extracts feature maps from the input image through a series of convolutional layers, capturing essential visual information. The neck component enhances these feature maps by combining multi-scale information, improving the detection of objects of varying sizes. Finally, the head component makes the final predictions by generating bounding boxes and classifying the detected objects. In our implementation of YOLOv5-s network, we use CSPDarknet as backbone to extract multi-dimensional features from the image, facilitating the detection of objects of various sizes. The deepen factor of our backbone is 0.33 and the widen factor is 0.5, controlling the number of layers in the network and the number of channels in the output feature map, respectively. The neck module employs a PAFPN (Path Aggregation Network with Feature Pyramid Network) with a deepen factor of 0.33 and a widen factor of 0.5, and channel numbers of [256, 512, 1024]. This component processes and fuses feature maps from different layers of the backbone, outputting a series of feature maps at various scales. The head module is a 3-layer convolutional network that converts these feature maps into outputs that include object presence, bounding box, and confidence levels within anchors.

After obtaining the bounding boxes of the mice, the process moves to the pose estimation stage. The pose\_hrnet\_w32 architecture typically consists of a backbone and a head module. We use HRNet [52] (High-Resolution Network) as the backbone, composed of 4 stages, processing feature maps of different resolutions through a multi-branch structure. The first stage has a branch with 4 Bottleneck blocks and 64 channels. In the second stage, two branches are introduced, with 48 and 96 channels, utilizing Basic residual blocks. The third stage further expands the network’s feature extraction capabilities with three branches having 48, 96, and 192 channels, respectively. Finally, in the fourth stage, the network has four branches, with channels increasing from 48 to 384. This multi-branch, multi-channel design allows HRNet to maintain high resolution while fully integrating multi-scale features, providing strong

feature support for pose estimation. The head of the model employs a Heatmap Head. This module’s main function is to convert the feature maps extracted by the backbone into heatmaps of keypoints, where each location on the heatmap corresponds to the probability of a keypoint. The Heatmap Head receives feature maps from the lowest resolution branch of HRNet, with 48 input channels, and uses a series of convolution operations to convert these feature maps into heatmap outputs of keypoints. Ultimately, the head outputs heatmaps with 24 channels, each corresponding to the probability distribution of a keypoint location. This design allows the Heatmap Head to effectively convert high-level feature maps into precise keypoint predictions, providing reliable positioning capabilities for pose estimation.

Given the substantial volume of data, we implemented parallelizable data loading, pre-processing, and post-processing features based on the original mmlab framework, utilizing high-performance CPUs and GPUs. This parallelization significantly accelerated training and reduced the computational cost associated with processing large video datasets.

### ***Training Details of 2D Kinematics Estimation Network***

For the 2D mouse detector, mmyolo, we used the SGD optimizer with a learning rate (lr) of 0.001, momentum of 0.937, and weight decay of 0.0005. To further optimize the training process, we implemented a linear dynamic learning rate strategy, with the lr factor set to 0.01, which means that the learning rate will gradually decrease linearly to 1% of the original learning rate as the number of training epochs increases. These settings enable the optimizer to gradually adjust the learning rate during training, improving the model’s convergence speed and final performance.

For the 2D mouse pose estimator, mmPose, we used the Adam optimizer with an initial learning rate (lr) of  $5e-4$ . The learning rate schedule consisted of two parts: first, a linear learning rate adjustment (LinearLR) was used for warm-up, with a start factor of 0.001, beginning from the 0th epoch and continuing until the 200th epoch. After the warm-up, a multi-step learning rate adjustment strategy (MultiStepLR) with a gamma parameter of 0.1 was employed. This combination strategy allows the model to gradually increase the learning rate in the early stages and then decay the learning rate during critical training stages, enhancing the model’s stability and accuracy.

To ensure the generalization performance of the model, we reserved the first five minutes of data from each video in the dataset as the test set. The remaining data was divided into training and validation sets in an 8:1 ratio. The training set was utilized for optimizing model parameters, the validation set for selecting the optimal model, and the test set for evaluating the final model’s generalization capability. This partitioning strategy ensures data independence across different stages, thereby reducing the potential for model overfitting.

We conducted the training using an NVIDIA RTX 4090 24GB. The mmyolo training lasted for 200 epochs, taking approximately 11 hours, while the mmPose training also lasted for 200 epochs and took around 11 hours.

### ***Error Metrics***

During training, the mmyolo framework separately computed object loss and bounding box loss using Cross-Entropy Loss. Given that our dataset contains only a single class (mice), class loss was not calculated. We assigned weights of [1.0, 0.05] to the object loss and bounding box loss, respectively, to achieve more effective joint optimization. In the mmpose framework, we computed MSE Loss of keypoints, which supervises the proximity of keypoints derived from the heatmap to the ground truth (GT).

In evaluating the two-stage pose estimation, we primarily utilized Average Precision (AP) and mean Average Precision (mAP) as performance metrics, alongside PCKAccuracy to assess performance on the test set. Our approach achieved pixel-level accuracy on 4K images.

Model performance was predominantly assessed using the metrics of AP and mAP. AP measures the accuracy of predictions for individual keypoints, whereas mAP provides an overall evaluation of accuracy across all keypoints. Additionally, we monitored the evolution of the loss function to evaluate training progress and convergence.

### ***3D Pose Triangulation***

To accurately capture the three-dimensional motion trajectories of mice, we employed the Easymocap [53] library, integrating camera parameters with the two-dimensional coordinates of keypoints detected from  $n$  distinct camera perspectives (in our study,  $n=8$ ). This setup employed a sophisticated triangulation methodology essential for the precise reconstruction of the spatial positions of these keypoints. The core of our approach is anchored in the optimization of the triangulation equations derived from combining each camera’s viewpoint:

$$\arg \min_{(x,y,z)} \sum_{i=1}^n \left\| (u_i, v_i) - \frac{P_i(x, y, z, 1)}{P_{i,3}(x, y, z, 1)} \right\|_2 \quad (1)$$

where  $P_i$  denotes the projection matrices corresponding to each of the eight camera angles and  $P_{i,3}$  refers to the third row of the projection matrix, which is used to normalize the homogeneous coordinates after projection.  $(u_i, v_i)$  represent the image coordinates of the keypoints. Our methodology synthesizes data across all camera angles, leveraging the collective information to compute the most probable three-dimensional coordinates  $(x, y, z)$ . This multi-view triangulation approach minimizes spatial uncertainties and refines the accuracy of the positional data.

Utilizing data from multiple perspectives substantially enhances the robustness and reliability of the tracking system. This approach not only augments the spatial resolution of the reconstructed keypoints but also offers a more detailed and nuanced analysis of mouse behaviors, which is pivotal for sophisticated behavioral studies. The comprehensive coverage provided by multiple camera angles significantly reduces occlusions and ambiguities, delivering clearer and more actionable insights into the intricacies of animal movement dynamics.

### ***3D Velocity Calculation***

The 3D keypoint data are used as input for the 3D velocity calculation process, including the keypoint positions of the mouse at each frame, stored in .json format.



For the  $j$ -th keypoint position  $k_i^j \in \mathbb{R}^3$  at frame  $i$ , captured under frame rate  $fps$ , the  $j$ -th keypoint’s velocity at frame  $i$ ,  $\mathbf{v}_i^j \in \mathbb{R}^3$ , is calculated as follows, representing the mean velocity of the keypoint from the previous frame to the current frame:

$$\mathbf{v}_i^j = \frac{k_i^j - k_{i-1}^j}{fps} \quad (2)$$

In order to demonstrate the trend of the movements in a more obvious way, we convert the velocities in reference to the overall mouse movement using direction vector  $d^{base} \in \mathbb{R}^3$  defined by keypoints strategically chosen:

$$d^{base} = k_i^5 - k_i^6 \quad (3)$$

where  $k_i^5$  (SpineG) and  $k_i^6$  (SpineH) denote the 3D coordinates of the 5-th and 6-th keypoints at frame  $i$ .

The converted velocity  $v_i^j \in \mathbb{R}$ , is a scalar representing the magnitude of the keypoint velocity  $\mathbf{v}_i^j$ , with the sign indicating the relative tendency of the movement. It is computed as:

$$v_i^j = \text{sign} \left( \arccos \left( \frac{\mathbf{v}_i^j \cdot d^{base}}{\|\mathbf{v}_i^j\| \|d^{base}\|} \right) - \frac{\pi}{2} \right) \cdot \|\mathbf{v}_i^j\| \quad (4)$$

### ***Automated Open-vocabulary Behavior Annotation***

We collect a behavior dataset with open-vocabulary annotations using GPT-4o (gpt-4o-2024-05-13). Specifically, we extract images at 5 frames per second from all of our video, utilizing images from two mutually perpendicular viewpoints. We concatenate the two images horizontally as input to GPT-4o. We then generate the prompt with speed information to acquire detailed descriptions of mouse behavior.

An example prompt is as follows:

The user will show you one frame of a photo or several photos of a mouse in a glass chamber shot at different views at the same time, and necessary information such as the absolute value of velocity, etc.. You need to give me the description of the motion of the mice in the photos. You should give me a .json format, where there are several elements. You should describe the motion of the mouse in each part of json using full sentences as detailed as possible. You should answer each of the following questions. Your response should include but not limited to information of below questions. The first element in the json is "Overall". From the images, what is the overall status of the mouse, stationary or in motion? If it is moving, the movement is slow, moderate or rapid? What is this mouse doing? Is it standing, walking, or doing nothing?Next element: "Head". It should be the description of the head and face region. What can you see from its face? Is it just looking around? Or is it licking / grooming its paw or fur? What is the head position and orientation with respect to its body or

the ground? Is the head turning left, turning right or upward? Which direction is it looking into? Next element: "Limb". What is its front paw / front foot doing? Is it on the ground or in the air? What is its hind paw / hind leg doing? Is it on the ground or in the air? Is it clearly walking? What is its tail doing? Is it extended on the ground, in the air parallel to the ground or pointed upwards? Next element: "Torso". What can you see from its main body, or torso? Is the spine curved vertically, horizontally, or stretched? Are the chest, abdomen and hip (or butt) partially contacted with the ground, fully lay on the ground, or in the air? Next element: "Others". What else can you directly see about the motion or behavior of this mouse in this photo? Please include other information and describe it as detailed as possible, but still the description should be facts, rather than opinions or assumptions. And the last element would be the "Keywords". You should use line of keywords separated by commas to conclude and summarize the identifiable features of the mouse behavior in each of the above components. Note that your description / keywords should only be about the animal itself, without the environments. And your answers should only contain facts, without opinions or assumptions. Do NOT use negative sentence such as "rather than", or "instead of". The main part of the description should come from the image, and the speed data is only used as an auxiliary. The velocity is an absolute value without direction, so a high velocity does not necessarily mean the mouse is walking or running, it might just be caused by vertical movement of the body, such as standing up. And the value of velocity is only an estimate with noise, so a low value such as 1 cm/s might be only caused by noise or shaking of the mouse, instead of the actual movement, a high value might also be caused by a detection failure. Thus, the major conclusion should only come from the images themselves, and the velocity is only a cross-validation. Also, do NOT include exact number of speed in your response, use natural language to describe it instead. The first two photos were shot at different views at the same time. The overall movement speed of the mouse is: 2.49 cm/s, the speed of the head: 5.18 cm/s, speed of left and right forelimbs: 17.18, 19.87 cm/s, and left and right hind limbs are 3.38, 2.63 cm/s respectively.

We access the GPT-4o API through Microsoft Azure to generate our dataset. This dataset encompasses 15 hours of video, from which 270085 frames have been selected. For each selected image, we generated 3D keypoints, velocity data, and a detailed textual description using GPT-4o, alongside annotations regarding the mice's modeling and drug use. The same prompts and descriptions will later be utilized to train our Vision-Language Model.

An example answer is as follows:

```
{ "Overall": "The mouse is in motion, exhibiting a moderate movement speed. It appears to be standing on its hind legs and interacting with the glass chamber.", "Head": "The mouse's head is oriented
```

```
upward, looking towards the top of the glass chamber. It is not engaged in grooming or licking.", "Limb": "The front paws are in the air, reaching towards the glass. The hind paws are on the ground, supporting the mouse's body. The tail is extended on the ground.", "Torso": "The torso is vertically stretched, with the spine aligned vertically. The chest, abdomen, and hip are elevated and not in contact with the ground.", "Others": "The mouse is actively engaging with its environment, possibly exploring or attempting to climb the glass chamber.", "Keywords": "motion, standing, head upward, front paws in air, hind paws on ground, tail extended, torso vertical, exploring"}
```

### ***Dataset Curation***

To ensure that the outputs generated by GPT-4o conform to a strict JSON format, which is essential for subsequent readability and processing, we have developed a robust JSON validation method. Initially, we capture the response from OpenAI as a raw string, allowing us to apply regular expressions effectively. This approach enables us to search for and extract the content enclosed within the JSON object, thereby filtering out any responses that do not meet the required format. By focusing on this precise extraction process, we can systematically eliminate improperly formatted data before it reaches the next stage of our workflow.

Once we have validated the JSON outputs, we further enhance the quality of our dataset by employing a faster LLM model, specifically GPT-4o mini, to score all generated JSON files. In this phase, we provide both the generated JSON results and the corresponding input images to the model, prompting it to evaluate critical aspects such as accuracy, coherence, and relevance and scoring them from 0 to 10. The evaluation process is guided by specific criteria that help ensure the data meets our standards for training purposes. Consequently, any entries that receive the lowest scores are removed from the training dataset, allowing us to refine our data and improve the overall quality of our training inputs. This dual-layer validation process not only strengthens the integrity of our dataset but also enhances the performance of our models in subsequent training phases.

## **4.3 Model Architecture and Training Details**

### ***Training Our Model with the SWIFT Framework***

Our model is trained using the Scalable lightWeight Infrastructure for Fine-Tuning (SWIFT) framework, a comprehensive solution designed for training, inference, evaluation, and deployment of Large Language Models and Vision-Language Models. SWIFT allows us to train models of different architectures in the same training manner. In addition, SWIFT supports various third-party optimization libraries for training and deployment. In our practice, we use DeepSpeed to accelerate the model for multi-GPU training and LMDeploy to accelerate the model for deployment on multiple GPUs.

We registered the aforementioned dataset as the training dataset within the SWIFT framework and utilized it to train two distinct models: InternVL2-Llama3-76B and MiniCPM-V-v2.6-chat.

### ***Model Architecture***

We present two distinct models in our work, MouseGPT-Large, and MouseGPT-Lite. The first and most powerful Large Model, leveraging InternVL2-Llama3-76B [38, 54], is a Vision-Language Model (VLM) comprising 76 billion parameters. The model demonstrates superior performance in multi-modal tasks, offering advanced capabilities in handling diverse data and delivering accurate results.

The model architecture consists of three main components. First, the vision module employs a query-key-value (qkv) attention structure [55] to process visual inputs. This module transforms images into a high-dimensional feature space, capturing spatial and contextual information. Second, the language module utilizes the Llama [56] for Causal Language Modeling (LlamaCausalLM) architecture, designed for efficient text generation and understanding. Finally, the integration module bridges the vision and language outputs, combining the two modalities to facilitate coherent inference across both visual and textual inputs.

1. **Vision Module.** The vision processing module is designed for high-capacity visual tasks, starting with a convolutional patch embedding layer. This layer processes input images (typically  $448 \times 448 \times 3$ ) by dividing them into patches using a  $14 \times 14$  kernel and a stride of 14. Each patch is then projected into a 3200-dimensional feature space, resulting in a grid of  $32 \times 32$  patches, each represented by a 3200-dimensional feature vector. The encoder consists of 45 layers, each containing a multi-head self-attention mechanism, which projects the input features (3200 dimensions) into a higher 9600-dimensional space for queries, keys, and values (QKV). After attention calculations, the outputs are projected back to 3200 dimensions. Following the attention mechanism, a multi-layer perceptron (MLP) transforms the 3200-dimensional features by first expanding them to 12800 dimensions and then reducing them back to 3200 dimensions. This is done using two linear layers, with GELU activations applied between them. The outputs of both the attention and MLP components are followed by a normalize layer and dropout layer.
2. **Language Module.** The language processing component handles natural language tasks by embedding input tokens into an 8192-dimensional space. The language model consists of 80 layers, each equipped with a self-attention mechanism that projects the 8192-dimensional input features into query, key, and value spaces. The key and value projections are reduced to 1024 dimensions, while the query remains at 8192 dimensions. The attention output is projected back to 8192 dimensions. The MLP following the attention mechanism expands the 8192-dimensional features to 28672 dimensions before reducing them back to 8192 dimensions using three linear layers with SiLU activations. Layer normalization is applied after both the attention and MLP operations.
3. **Integration and Multi-Modal Processing.** To seamlessly combine visual and language information, an additional multi-layer perceptron (MLP) is used to fuse the outputs from the vision and language modules. The visual features (3200-dimensional) and language features (8192-dimensional) are concatenated, resulting in a 12800-dimensional vector. This vector is then passed through a linear transformation that reduces the dimensionality to 8192, enabling effective fusion of the

two modalities. Another linear layer is applied to maintain the dimensionality at 8192, ensuring consistency in the fused feature representation. Layer normalization is applied to the integrated features to maintain coherent distributions during multi-modal processing.

The second lightweight model, MouseGPT-Lite, utilizes MiniCPM-V-v2.6-chat [39] and is a Vision-Language Model (VLM) with 8 billion parameters, approximately one-tenth the size of our MouseGPT-Large. This model effectively balances powerful analysis capabilities with enhanced inference speed, making it ideal for use in resource-constrained environments.

The architecture consists of three key components. The language module is based on the Qwen2ForCausalLM model [57], which provides robust language processing capabilities optimized for efficiency. The vision module employs the SigLIP model [58], designed for high-performance visual feature extraction. These two modules are integrated using a Resampler, which combines the outputs of both the vision and language components.

Specifically, the network structure can be divided into the following components:

1. Text generation Module. The text generation module is based on a transformer model that operates within an encoder-decoder framework. The encoder consists of 28 layers, each employing a multi-headed attention mechanism, which projects the input features (3584 dimensions) into higher-dimensional spaces for queries, keys, and values. The attention outputs are passed through a multi-layer perceptron (MLP), consisting of two linear transformations. The first transformation expands the 3584-dimensional features to 18944 dimensions, while the second reduces them back to 3584 dimensions. These encoder and decoder layers are activated using the SiLU function and are regularized by a normalization layer.
2. Vision Processing Module. The vision processing module is based on a vision transformer that includes 27 layers for processing visual input. Each layer contains a multi-head attention mechanism, projecting the 1152-dimensional visual features into higher-dimensional spaces for queries, keys, and values. The attention outputs are processed through an MLP, which expands the features from 1152 dimensions to 4304 dimensions before reducing them back to 1152 dimensions. This process is regulated by LayerNorm and activated using a GELU-Tanh function, ensuring non-linear transformations of the visual features. The vision module employs a patch-based embedding system, where the input image is divided into patches using a  $14 \times 14$  kernel, embedding each patch into an 1152-dimensional feature space.
3. Integration and Resampling. The integration module plays a critical role in bridging the gap between the outputs of the text and vision processing modules. A resampler module is employed to align the feature dimensions from the two modalities. It utilizes a multi-head attention mechanism to resample the visual features (1152 dimensions) and align them with the text-based features (3584 dimensions). The resampled features are then fused, and a normalization layer ensures that the output features from both the text and vision modules are consistently integrated, facilitating seamless multi-modal processing.

### *Training Details*

We train our Vision-Language Models (VLMs) using a multi-node distributed setup across 4 nodes, each equipped with 8 NVIDIA A100 GPUs. To optimize training, we use DeepSpeed [59] for efficient distributed operations and employ mixed-precision (bfloat16) to reduce memory usage and improve computational speed. Communication and gradient updates are coordinated using PyTorch’s torchrun utility.

The AdamW optimizer is used with a learning rate of 1e-5, following a cosine decay schedule with a warmup ratio of 0.05. Flash attention is applied to enhance the computational efficiency of attention layers, particularly for processing long sequences. To avoid padding and ensure maximum efficiency, we set the batch size to 1 for all training jobs.

Our models are trained on a custom dataset (See Dataset Overview), with 1% of the data reserved for testing. To align with standard Vision-Language Model (VLM) training protocols, we horizontally combine two images per sample and resize them to a resolution of 896×448. The InternVL2 model undergoes 18,000 iterations, while the MiniCPM model is trained for 45,900 iterations.

## **4.4 MouseGPT Behavior Analysis Framework**

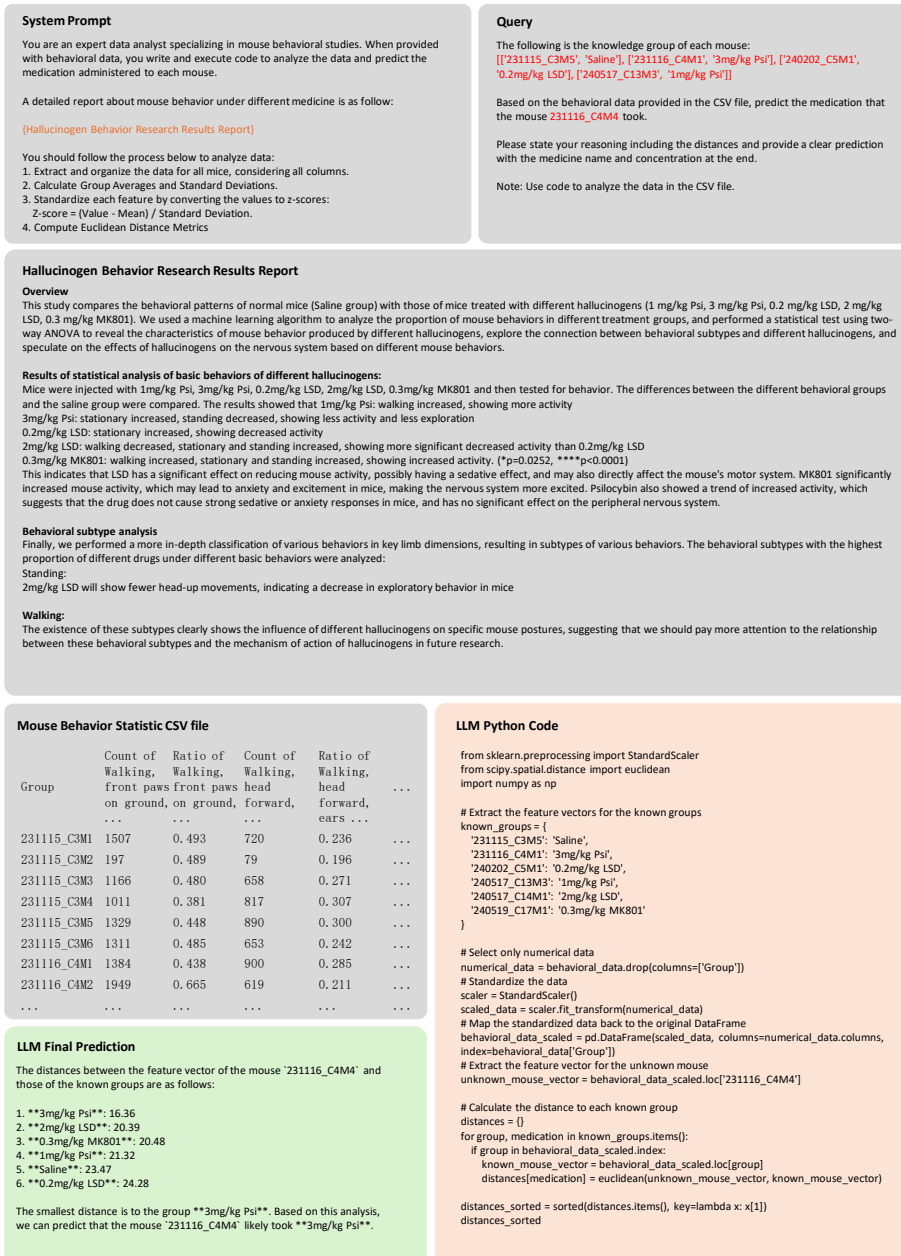
We designed the Advanced Behavior Analysis Framework to best work with our MouseGPT models, utilizing open-vocabulary text descriptions to facilitate comprehensive analysis of mouse behavior. This framework begins with data pre-processing and text embedding generation to convert open-vocabulary descriptions into computable features. It then integrates key components such as major behavior profiling, fine-grained behavior analysis, novel behavior discovery, behavioral phenotype prediction, and search capabilities, providing researchers with powerful tools to derive high-level insights and conduct detailed analyses effectively.

### *Data Pre-processing*

MouseGPT’s behavioral analysis framework is built on the detailed descriptions for each frame using a Vision-Language Model (VLM). In practice, we first sample frames from the multi-view videos and calculate the speed for each frame. Next, we apply a trained VLM to provide detailed behavioral descriptions for each sampled frame, enabling a comprehensive analysis of the mouse’s behavior.

To reduce computational overhead while preserving important behavioral information, we sample video frames at a rate of 5 frames per second (fps). Most of our video recordings are approximately 20 minutes long, and after sampling, this results in about 6,000 frames per video. This sampling rate is chosen to capture sufficient behavioral changes in the mouse’s movements without overloading the model with redundant frames. The velocity of the mouse (See Data Annotation and Curation) is derived from changes in the mouse’s position across consecutive frames, which is critical for understanding motion-based behaviors such as locomotion, exploration, and rearing.

For precise behavior tracking, we calculate the bounding box around the mouse using a trained 2D mouse detection neural network (See Data Annotation and Curation). The bounding box helps localize the mouse in each frame, facilitating the subsequent analysis. To ensure robust analysis, we select two orthogonal side views



**Extended Fig. 4 Example Procedure of Behavior Phenotype Prediction.** An illustrative example of the step-by-step process used by MouseGPT to predict the drug treatment administered to a mouse based on behavioral phenotype data. The procedure involves standardizing behavioral data, calculating Euclidean distances between feature vectors, and identifying the closest match among known treatment groups. This workflow highlights the integration of computational tools and statistical analysis to infer drug-induced behavioral effects with precision.

#### Query



"The user will show you one frame of a photo or several photos of a mouse in a glass chamber shot at different views at the same time, and necessary information such as the absolute value of velocity, etc.. You need to give me the description of the motion of the mice in the photos. You should give me a json format, where there are several elements. You should describe the motion of the mouse in each part of json using full sentences as detailed as possible. You should answer each of the following questions. Your response should include but not limited to information of below questions. The first element in the json is \"Overall\". From the images, what is the overall status of the mouse, stationary or in motion? If it is moving, the movement is slow, moderate or rapid? What is this mouse doing? Is it standing, walking, or doing nothing? \nNext element: \"Head\". It should be the description of the head and face region. What can you see from its face? Is it just looking around? Or is it licking / grooming its paw or fur? What is the head position and orientation with respect to its body or the ground? Is the head turning left, turning right or upward? Which direction is it looking into? \nNext element: \"Limb\". What is its front paw / front foot doing? Is it on the ground or in the air? What is its hind paw / hind leg doing? Is it on the ground or in the air? Is it clearly walking? What is its tail doing? Is it extended on the ground, in the air parallel to the ground or pointed upwards? \nNext element: \"Torso\". What can you see from its main body, or torso? Is the spine curved vertically, horizontally, or stretched? Are the chest, abdomen and hip (or butt) partially contacted with the ground, fully lay on the ground, or in the air? \nNext element: \"Others\". What else can you directly see about the motion or behavior of this mouse in this photo? Please include other information and describe it as detailed as possible, but still the description should be facts, rather than opinions or assumptions. \nAnd the last element would be the \"Keywords\". You should use line of keywords separated by commas to conclude and summarize the identifiable features of the mouse behavior in each of the above components. \nNote that your description / keywords should only be about the animal itself, without the environments. And your answers should only contain facts, without opinions or assumptions. Do NOT use negative sentence such as \"rather than\", or \"instead of\". The main part of the description should come from the image, and the speed data is only used as an auxiliary. The velocity is an absolute value without direction, so a high velocity does not necessarily mean the mouse is walking or running, it might just caused by vertical movement of the body, such as standing up. And the value of velocity is only an estimate with noise, so a low value such as 1 cm/s might be only caused by noise or shaking of the mouse, instead of the actual movement, a high value might also caused by a detection failure. Thus, the major conclusion should only come from the images themselves, and the velocity is only a cross-validation. Also, do NOT include exact number of speed in your respond, use natural language to describe it instead. \n\nThe first two photos shot at different view at the same time. The overall movement speed of the mouse is: 0.64 cm/s, the speed of the head: 2.07 cm/s, speed of left and right forelimbs: 0.93, 1.19 cm/s, and left and right hind limbs are 0.68, 0.68 cm/s respectively."

#### MouseGPT-Large

"Overall": "The mouse appears to be stationary or moving very slowly. It is sitting on its hind legs with its front paws raised, possibly grooming itself.",  
"Head": "The head is oriented forward and slightly downward. The mouse appears to be looking at its front paws, which are raised close to its mouth. The head is not turning significantly in any direction.",  
"Limb": "The front paws are raised and close to the mouth, suggesting grooming behavior. The hind paws are on the ground, supporting the body. The tail is extended on the ground behind the mouse.",  
"Torso": "The torso is upright with the spine slightly curved vertically. The chest and abdomen are not in contact with the ground, indicating the mouse is sitting on its hind legs.",  
"Others": "The mouse's ears are upright and alert. The overall posture suggests a grooming behavior, with the front paws raised and close to the mouth.",  
"Keywords": "stationary, grooming, head forward, front paws raised, hind paws on ground, tail extended, upright torso, alert ears"

#### MouseGPT-Lite

"Overall": "The mouse appears to be stationary or moving very slowly. It is sitting with its body close to the ground.",  
"Head": "The mouse's head is oriented forward and slightly downward. It appears to be grooming or licking its paw. The head is not turning significantly in any direction.",  
"Limb": "The front paws are raised and close to the mouth, indicating grooming behavior. The hind paws are on the ground, supporting the body. The tail is extended on the ground.",  
"Torso": "The torso is slightly curved horizontally. The chest, abdomen, and hip are partially in contact with the ground.",  
"Others": "The mouse's ears are upright, and its eyes are open. The overall posture suggests grooming behavior.",  
"Keywords": "stationary, grooming, head forward, front paws raised, hind paws on ground, tail extended, torso curved, ears upright, eyes open"

#### GPT-4o

"Overall": {"Status": "In motion", "Movement": "Moderate", "Activity": "Walking"},  
"Head": {"Description": "The mouse's head is facing forward and slightly to the left. The mouse appears to be looking into the distance.", "Orientation": "The head is oriented forward and slightly to the left with respect to the body.", "Position": "The head is in a neutral position with respect to the ground."},  
"Limb": {"Front Paw": "The left front paw is extended and in the air, while the right front paw is on the ground.", "Front Foot": "The left front foot is on the ground, while the right front foot is in the air.", "Hind Paw": "The left hind paw is on the ground, while the right hind paw is in the air.", "Hind Leg": "The left hind leg is on the ground, while the right hind leg is in the air.", "Walking": "The mouse appears to be walking with a moderate speed."},  
"Torso": {"Spine": "The spine is curved slightly upwards.", "Contact with Ground": "The chest, abdomen, and hip are partially contacted with the ground.", "Position": "The mouse is standing on all four limbs with a slight lean forward."},  
"Others": "The mouse appears to be focused on something in the distance, possibly exploring its surroundings. The movement is steady and controlled, indicating that the mouse is walking rather than running or standing still.",  
"Keywords": "walking, moderate speed, neutral head position, extended front paw, partially contacted with ground"

#### InternVL2-Llama3-76B

```
{} json
```

"Overall": "The mouse is stationary and appears to be grooming itself",  
"Head": "The mouse's head is oriented downward and slightly to the right, and it is licking its paw.",  
"Limb": "The mouse's front paws are raised and positioned near its mouth, while its hind paws are on the ground. The tail is extended on the ground.",  
"Torso": "The mouse's torso is upright, and its spine is slightly curved. The chest, abdomen, and hip are partially contacted with the ground.",  
"Others": "The mouse is engaged in grooming behavior, focusing on its paw.",  
"Keywords": "stationary, grooming, licking paw, head down, front paws raised, hind paws on ground, tail extended"

#### MiniCPM-2.6

"Overall": {"Status": "In motion", "Movement": "Moderate", "Activity": "Walking"},  
"Head": {"Description": "The mouse's head is facing forward and slightly to the left. The mouse appears to be looking into the distance.", "Orientation": "The head is oriented forward and slightly to the left with respect to the body.", "Position": "The head is in a neutral position with respect to the ground."},  
"Limb": {"Front Paw": "The left front paw is extended and in the air, while the right front paw is on the ground.", "Front Foot": "The left front foot is on the ground, while the right front foot is in the air.", "Hind Paw": "The left hind paw is on the ground, while the right hind paw is in the air.", "Hind Leg": "The left hind leg is on the ground, while the right hind leg is in the air.", "Walking": "The mouse appears to be walking with a moderate speed."},  
"Torso": {"Spine": "The spine is curved slightly upwards.", "Contact with Ground": "The chest, abdomen, and hip are partially contacted with the ground.", "Position": "The mouse is standing on all four limbs with a slight lean forward."},  
"Others": "The mouse appears to be focused on something in the distance, possibly exploring its surroundings. The movement is steady and controlled, indicating that the mouse is walking rather than running or standing still.",  
"Keywords": "walking, moderate speed, neutral head position, extended front paw, partially contacted with ground"

**Extended Fig. 5 Comparison of MouseGPT Behavior Understanding Model and Other Vision-Language Models.** A comparative result of behavior descriptions generated by MouseGPT-Large, MouseGPT-Lite, GPT-4o, InternVL2-Llama3-76B, and MiniCPM-2.6. The figure demonstrates the differences in descriptive detail, accuracy, and interpretability across models for key behavioral components such as overall activity, head orientation, limb positioning, and torso posture.



from the video recordings, which provide complementary perspectives on the mouse’s movements. These side views are crucial for capturing both lateral and vertical behaviors, enabling a comprehensive understanding of the mouse’s actions.

Given the sampled frames, we leverage trained MouseGPT model to automatically annotate the behavior descriptions for each frame. For each request, trained MouseGPT model provides both the overall behavior and fine-grained descriptions of specific body parts such as head, limbs, torso, and tail. This approach allows for detailed and contextually rich annotations, capturing the nuances of the mouse’s behavior. The detailed prompt and the specific output format for these annotations can be found in Data Annotation and Curation.

### ***Transform Texts into Computable Features***

To enable quantitative analysis in our framework, we designed a dual-approach to convert the descriptive texts generated by our MouseGPT Model into computable features, using text embeddings and Keyword Info-Cards.

First, we convert the textual descriptions into high-dimensional embedding vectors to calculate distances and similarities for applications such as search and clustering. By employing this text embedding approach, we converted the full text of the behavioral descriptions into continuous high-dimensional feature vectors. In our implementation, we use the text-embedding-3-large model [60], which is a text embedding model designed for capturing semantic meaning, to generate a 3072-dimensional embedding vector for each behavioral description. This semantic-aware embedding vector allows similar behaviors to have smaller distance metrics between their corresponding vectors, enabling more accurate comparisons in high-dimensional space.

We also developed a parallel keyword-based matching algorithm that leverages Large Language Models (LLMs). In addition to the fuzzy matching and unsupervised clustering capabilities enabled by high-dimensional text embeddings, the keyword info-card provides an exact matching functionality. Using an LLM, keywords are extracted from the behavioral descriptions and represented as a “bag-of-words” — an approach that captures key features of the text without considering word order. This bag-of-words representation forms a computable feature that allows for precise and efficient identification of behaviors, complementing the more flexible semantic embeddings with direct, interpretable metrics.

### ***Major Behavior Profiling - Clustering Implementation***

We designed an LLM-based clustering algorithm for major behavior profiling during behavior analysis, employing a two-stage approach to ensure minimal semantic overlap between clusters. In the first stage, clustering is performed based on vector distances in the embedding space, while in the second stage, a Large Language Model (LLM) refines these clusters by leveraging open-vocabulary descriptions. The final output assigns each behavior cluster a primary descriptive label.

In the initial clustering stage, distances between data points are calculated using cosine similarity, which measures the angular difference between vectors in the embedding space. These distances are then used as input to the Agglomerative Hierarchical Clustering algorithm from SciPy (using `scipy.cluster.hierarchy.linkage`),

constructing a dendrogram that provides a hierarchical structure of data points. The dendrogram helps determine how to iteratively merge clusters, using the shortest inter-cluster distance as a measure.

We define two critical hyperparameters: the target number of clusters  $\theta_c$  and the minimum number of elements per cluster  $\theta_e$ . We employ the **fcluster** algorithm from SciPy to cut the dendrogram and form  $\theta_c$  clusters. Clusters with fewer than  $\theta_e$  elements are reassigned to nearby clusters. If the conditions are not satisfied, the process is repeated with an increased number of initial clusters until  $\theta_c$  stable clusters are achieved.

In the refinement stage, we use an LLM to enhance the quality and semantic coherence of the clusters. First, the most frequently occurring keywords within each cluster are extracted, and the top five are retained as a preliminary label for the cluster. The LLM then evaluates whether similar clusters should be merged, based on their labels, to improve interpretability and ensure consistency in behavioral characterization. The LLM makes the final decision on merging clusters, allowing a flexible and data-driven adjustment of cluster boundaries.

This two-stage clustering method facilitates nuanced major behavior profiling by creating behaviorally meaningful groups, while leveraging natural language descriptions to improve cluster coherence and accuracy. It allows researchers to explore both overarching patterns and subtle distinctions in mouse behavior, contributing to a more complete understanding of behavioral phenotypes (Extended Fig. 6).

### ***Fine-Grained Behavior Analysis - LLM-Guided keyword matching***

We developed an LLM-guided keyword-matching method to effectively quantify and summarize fine-grained behavioral descriptions of mice. This approach allows for detailed tracking of body part movements, capturing subtle variations in behavior that are essential for comprehensive behavior analysis.

For this purpose, we maintain a Python dictionary for each key body part: “Torso”, “Head”, and “Limb”. Each dictionary consists of predefined behaviors (as keys) and associated textual descriptions (as values). For instance, in the “Torso” dictionary, keys such as “upright”, “horizontally stretched”, and “curved” categorize different postures, with corresponding values detailing specific descriptions of these behaviors.

To perform fine-grained behavior analysis, we process the frame-by-frame textual descriptions and attempt to match each description with the dictionary entries using regular expression matching. If a match is found, we annotate the behavior for that frame using the corresponding key from the dictionary. For any behavior descriptions that do not match existing entries, we pass the description to the LLM, which either assigns it to an existing key (if semantically similar) or generates a new key, thus updating the dictionary dynamically. This enables continuous learning and expansion of the behavior lexicon as more nuanced behaviors emerge.

By counting the occurrences of these keys across video frames, we can quantitatively track specific behaviors over time, providing a comprehensive and dynamic analysis of fine-grained behaviors throughout the video sequence (Extended Fig. 7).

---

**Algorithm 1** Two-Stage Behavioral Clustering with LLM Refinement

---

```
1: Input:  
    • Description embedded vector list:  $V = \{v_1, v_2, \dots, v_n\}$   
    • Description keyword list:  $T = \{t_1, t_2, \dots, t_n\}$   
2: Hyperparameters:  
    • Desired number of clusters:  $\theta_c$   
    • Minimum number of elements per cluster:  $\theta_e$   
3: Initialization:  
    • Cluster ID for each frame:  $C$   
    • Keyword list for each cluster:  $K$   
    • Construct linkage matrix:  $lm = \text{construct\_linkage\_matrix}(V)$   
    •  $current\_cluster\_num \leftarrow 0$   
4: while  $current\_cluster\_num < \theta_c$  do  
5:    $C \leftarrow \text{fcluster}(lm, \theta_c)$   
6:    $cluster\_elem\_num \leftarrow \text{unique}(C)$   
7:    $current\_cluster\_num \leftarrow \text{len}(cluster\_elem\_num) - 1$   
8:   for each cluster  $i$  in  $cluster\_elem\_num$  do  
9:     if  $i = -1$  then  
10:      continue  
11:    end if  
12:    if  $\text{len}(C[C == i]) < \theta_e$  then  
13:       $C[C == i] \leftarrow -1$   
14:       $\theta_c \leftarrow \theta_c + 1$   
15:       $current\_cluster\_num \leftarrow current\_cluster\_num - 1$   
16:    end if  
17:  end for  
18: end while  
19:  $K \leftarrow \text{union\_keywords}(T, C)$   
20:  $C \leftarrow \text{LLM\_merge}(K, C)$   
21: Output: Final cluster assignments  $C$ 
```

---

***Novel Behavior Discovery - Anomaly Detection***

We employ an LLM-based Novel Behavior Discovery method, using anomaly detection algorithms to identify rare or previously unobserved behaviors within a sequence of videos. These rare events, such as a mouse jumping in just 1 or 2 frames in a 10,000-frame-length video sequence, can reveal subtle behavioral patterns that human observers are likely to miss and other machine learning methods may overlook due to noise. For this, we applied the Isolation Forest algorithm to the embedded vectors representing behavior descriptions of each frame.

The Isolation Forest algorithm works by randomly sub-sampling vectors and constructing an ensemble of isolation trees. Each tree is trained on a subset of vectors, and

---

**Algorithm 2** Fine-grained Behavioral Classification for Body Parts

---

```
1: Input:  
   • Description list  $T = \{t_1, t_2, \dots, t_n\}$   
2: Initialization:  
   • Python Dictionary for each body part:  $D_{\text{Head}}, D_{\text{Torso}}, D_{\text{Limb}}$   
   • Fine-grained behavioral description for each frame:  $F = \{F_1, F_2, \dots, F_n\}$   
3: for  $D_j \in \{D_{\text{Head}}, D_{\text{Torso}}, D_{\text{Limb}}\}$  do  
4:   for  $t_i \in T$  do  
5:      $is\_matched \leftarrow \text{False}$   
6:     for  $key_k \in D_j.keys$  do  
7:       for  $value_v \in D_j[key_k]$  do  
8:         if regular-expression-matching( $value_v, t_i$ ) is True then  
9:           Append  $key_k$  to  $F_i$   
10:           $is\_matched \leftarrow \text{True}$   
11:         end if  
12:       end for  
13:     end for  
14:     if  $is\_matched = \text{False}$  then  
15:        $key_{\text{new}} \leftarrow \text{ask\_LLM\_for\_behavior\_label}(t_i, D_j.keys)$   
16:        $D_j[key_{\text{new}}] \leftarrow t_i$   
17:     end if  
18:   end for  
19: end for  
20: Output: Fine-grained behavioral description list  $F$ 
```

---

the algorithm isolates rare behaviors more effectively through these random splits. As these behaviors are distinct, they are more likely to appear as isolated nodes within the trees. Rare behaviors are thus identified by detecting isolated samples, where behaviors with fewer splits indicate a lower frequency.

We tuned two critical hyperparameters: the number of estimators and the contamination rate, which together control the sensitivity of the model to rare events. In our implementation, we set these parameters to 100 and 0.0001, respectively, balancing the detection sensitivity and the noise level to achieve optimal results. By using this approach, we ensure that rare but significant behavioral anomalies are captured, facilitating novel behavior discovery and advancing our understanding of nuanced behavioral phenomena in mouse models.

### ***Behavioral Phenotype Prediction***

Our Behavioral Phenotype Prediction framework utilizes a large language model (LLM) to analyze behavioral reports of mice, enabling the determination of the administered drugs with high precision (Extended Fig. 4).

First, we constructed a “knowledge base” for the LLM, consisting of two components that provides essential background knowledge for effective behavioral phenotype

analysis. The first component is the Expert Experience Database, containing academic materials and reports written by experts based on existing knowledge and statistical data of characteristic behavioral changes in mice following specific drug injections or particular experimental procedures, ensuring the reliability of this information.

The second component is the Multi-layer Behavior Report documenting behaviors observed in a sample mouse for each experimental condition, such as drug injections, collected during controlled experimental sessions. This table includes Major Behavior Profiling results like walking and rearing, as well as fine-grained behavior details such as instances of head-up movements during walking. Also, a report documenting novel behavior happened during the experiment is presented. The Behavior reports, together with the Expert Experience Database, are provided to the LLM as system prompts.

Next, we supply the LLM with another Multi-layer Behavior Report of a test subject under specific experimental conditions, and prompt it to infer the drug administered based on the knowledge base, using its ability to interpret behavioral patterns and match them with existing data in the knowledge base. During this analysis, the LLM extracts relevant data from the database and generates python code (see Natural Language User Interface) to identify the mouse with the closest behavior distribution in the knowledge base of each behavioral phenotype. When assessing behavioral similarities, the LLM calculates scores to determine the closest matching behavioral category, dynamically adjusting the weighting of various behaviors based on insights from the expert report.

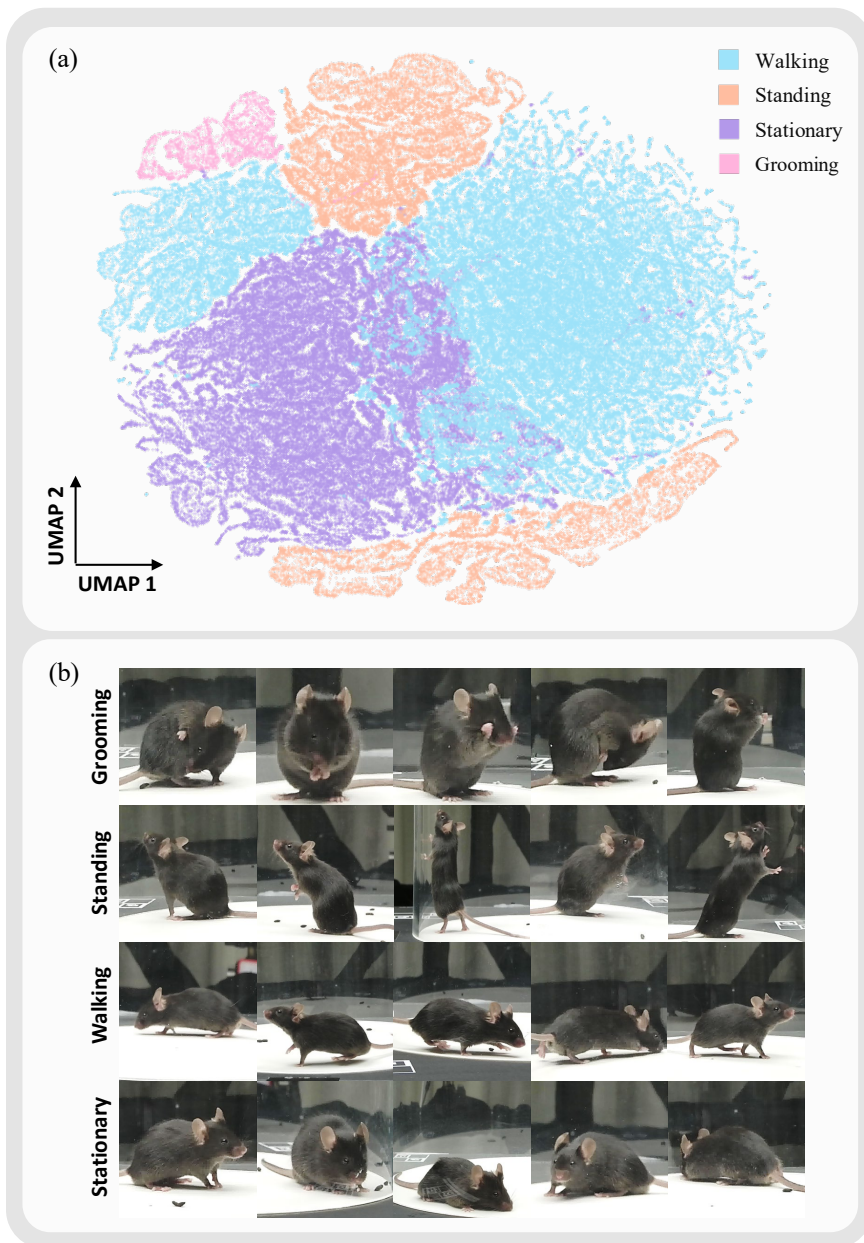
### *Search*

We designed a natural language search method that allows users to locate specific behaviors in video sequences, leveraging the subtle nuances that natural language descriptions provide compared to single-word labels. This search approach utilizes fuzzy matching based on embedding distances, ensuring that even slight variations in behavior can be identified. Users can describe behaviors of interest by inputting either a single word, like “rear up”, or a detailed phrase such as “mouse standing on hind legs”.

We embed the user’s input into a high-dimensional vector using the same embedding model, text-embedding-3-large, and calculate cosine similarity with each frame’s embedded vector. Frames corresponding to the top N vectors with the highest similarity scores are returned, ensuring users receive the most relevant results. This approach leverages natural language descriptions to intuitively match and locate the desired frames, enhancing the user experience.

## **4.5 Behavior analysis and statistic**

All statistical analyses of hallucinatory behaviors were completed on GraphPad Prism 8.0. We selected mice treated with Saline, 2 mg/kg Lysergic acid diethylamide (LSD), 0.3 mg/kg MK-801, and 3 mg/kg Psilocybin (n=5,4,5,6 respectively) from the dataset to showcase differences in hallucinogen-induced behavioral phenotypes. The hallucination dataset also includes three groups that did not participate in the statistical analysis: 1mg/kg Psilocybin (n=4), 10mg/kg Psilocybin (n=2), and 0.2mg/kg LSD (n=5). For each mouse, MouseGPT processed 6000 images at a time resolution of 5



**Extended Fig. 6 Identification of the major behavior by MouseGPT.** (a) UMAP visualization of the behavioral description embeddings from the hallucination dataset, colored by major behavior categories that are summarized by MouseGPT. (b) Representative example of each behavior category

fps to identify behavioral categories. After obtaining the categories of primary behaviors and posture-based behavior subtype, we calculated the proportion of various main behaviors within 20 minutes for each mouse, as well as the proportion of fine behaviors within walking behavior. Two-way ANOVA was used to test the significance of differences. For the temporal and spatial distribution corresponding to each type of behavior, we used custom Python scripts for plotting. To allow MGPT to learn the behavioral phenotypes of various drugs and make predictions for given mice, we randomly selected one mouse from each category and input its behavioral results into the model, then had the remaining mice predict the category they might belong to.

## 4.6 Natural Language User Interface

Our natural language user interaction is facilitated through an Agent that integrates multiple Vision-Language Models and a customizable toolset. Users can seamlessly perform tasks like mouse behavior analysis, including search, clustering, and more, all through natural language commands. Additionally, the Agent can automatically generate and execute code to help users complete statistical analyses. (Extended Fig. 2)

We build our Agent on the LangChain [43], a framework designed for building applications that integrate large language models as agents with external tools. The Agent processes complex user commands by breaking them down into executable steps, invoking the appropriate tools or models in sequence. This approach allows users to interact with the system intuitively, while the Agent efficiently manages the underlying complexity.

The system prompt used to create the Agent is shown below:

```
1 instructions = """You are a research assistant specializing in mouse behavior
2   analysis. Your next task is to assist me in analyzing a mouse video using the
3   available tools.
4   You have access to a Python REPL for executing code. When writing code, begin by
5   reading the necessary files from the database, followed by reviewing the table
6   headers to confirm the structure and content. This will help you avoid issues
   like key errors.
   If you encounter any errors, debug the code and retry until successful.
   """
```

**Listing 1** Python Example

### *Workflow Design*

1. **User Prompt:** At the beginning of each round, the user sends a prompt to the agent through the dialog box. The agent could receive both the prompt and the frame ID that the user is analyzing, which ensures that the agent has context regarding the specific frame.
2. **Tool Invocation Decision:** Upon receiving the prompt, the agent analyzes the input to determine whether a tool invocation is required to answer the user's request. If necessary, the agent formulates a tool request, which includes specific parameters such as the frame ID, relevant data, and task requirements, and waits for the tool to return results.

3. **Tool Execution and Data Processing:** Once the tool receives the request, it accesses the local data (e.g., video frames or experimental results) and performs the corresponding calculations or analyses. The detailed results generated by the tool are saved as a file for later access. Meanwhile, a summarized version of the results is returned to the agent in text form.
4. **Response to User and Logging:** The agent then returns a detailed answer to the user, incorporating the summarized results from the tool. Simultaneously, the detailed results, including tool invocations and intermediate calculations, are logged and presented in the interface’s logging section. This ensures transparency in the workflow, allowing users to review the exact process and results of the tool invocations.

### *User Interface*

We implemented the user interface using Gradio [61], creating an accessible and interactive environment for users to engage with the Vision-Language Model (VLM). After importing the pre-processed data, users can utilize our natural language interface to conduct further analysis. The interface is organized into the following main sections:

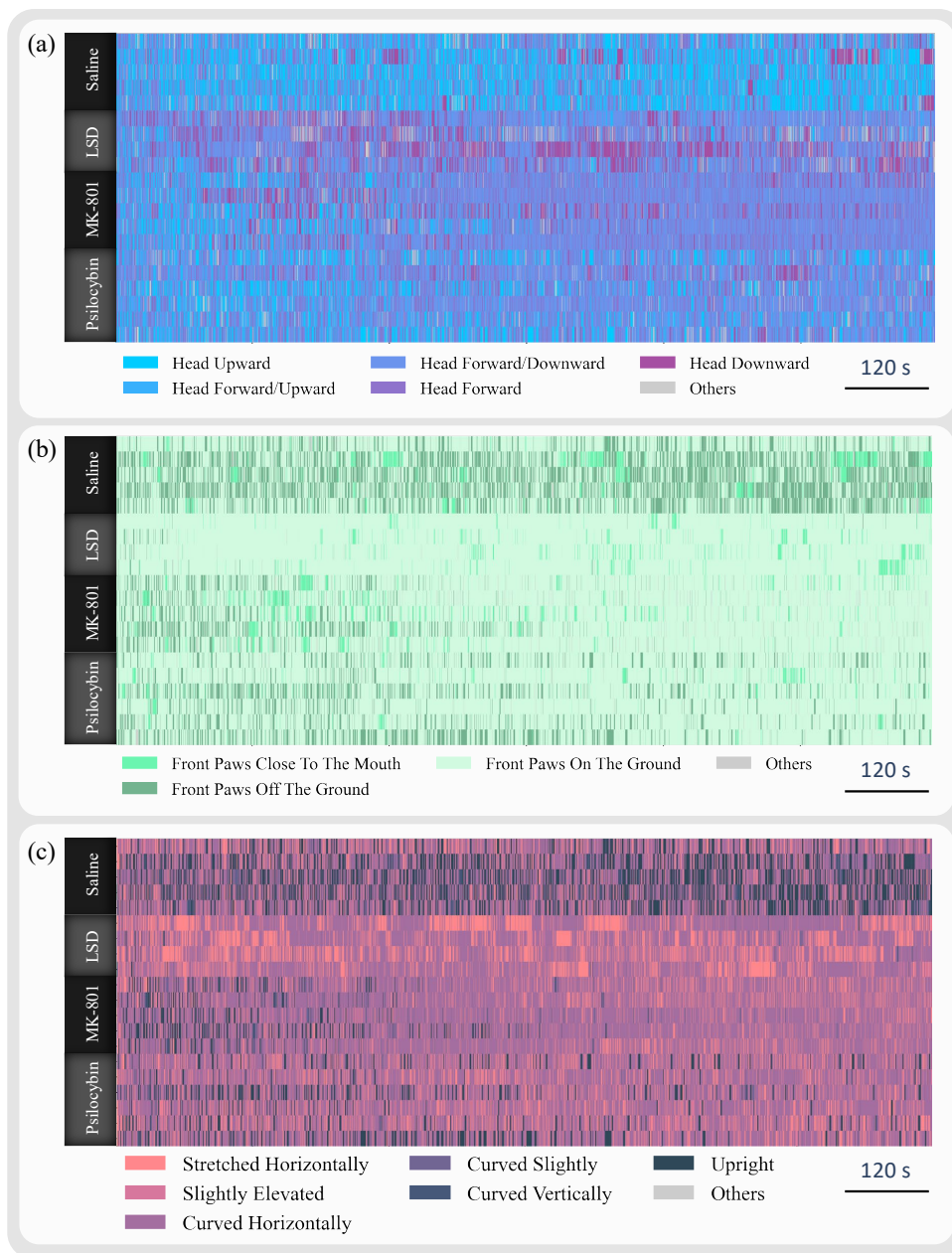
1. **Dialog Box.** This section allows the user to interact with the Agent by typing queries. Users can ask for various tasks, such as analyzing a specific data frame or requesting classification for the video.
2. **Video Frame Preview and Slider.** Users can navigate video content using the frame preview and slider feature. By dragging the slider, users can select a specific frame for inspection. During the conversation, the Agent automatically detects the currently selected frame.
3. **Record of Tool Invocation.** This section provides a clear overview of how the Agent employs various tools, displaying the input and output of each tool as well as intermediate results. Users can also export results, such as clusters and generated code, using the data packaging functions integrated into the interface.

### *Tools Integration*

Tools integration allows interaction between the LLM-based Agent and various mouse analysis tools. We utilize LangChain’s `langchain_core.tools` to incorporate the major behavior profiling, novel behavior discovery, search, and classification functions described in Section 4.3 into tools that can be invoked by the Agent.

Each tool is meticulously designed with clearly defined input and output formats, as well as variable types, ensuring seamless communication between the Agent and the tools. Additionally, we provide a detailed description for each tool, allowing the Agent to fully understand the tool’s functionality and usage scenarios. To streamline the process, we summarize the results after they are computed by the tools and return these summaries to the Agent. For example, in the classification and clustering functions, we summarize the percentage of occurrences for each behavioral classification. For the search and novel behavior discovery functions, we return the specific frame IDs along with the corresponding behaviors to the Agent.





**Extended Fig. 7 Temporal occurrence pattern of fine-grained pose in four groups.** (a)-(c), Ethogram displays the posture characteristics of all mice in each of the four groups at every moment within the 20-minute recording interval, from the three dimensions of Head, Limbs, and Torso.

Here is an example of a description of the tool, used to explain the purpose and input/output format of the tool to the agent:

```
1 @tool
2 def tool_search(behavior_description: str) -> dict:
3     """
4     A search tool for behaviour. Based on the behaviour description entered by the
5     user, search for the frame index corresponding to the closest behaviour
6     description among all the data. return the five closest frame indexes, and
7     sort and save the closeness of all the frames.
8
9     Input param:
10    - behavior_description: Description of target behaviour
11
12    Output:
13    - a dict
14      {
15        "top_5": a list with 5 frame index
16        "save_path": str, the paths of the searching result
17      }
18    """
```

**Listing 2** Python Example

To meet the users' more specific requirements, such as "counting the frequency of transitions between certain behaviors", we integrated the Python toolkit `langchain\experimental.utilities.PythonREPL`. The Python REPL (Read-Eval-Print Loop) is an interactive programming environment that allows the Agent to input Python code and execute it immediately. This tool enables the Agent to write and execute custom Python code in a virtual environment, providing access to local data and facilitating more complex calculations. The REPL operates by following these steps: it reads a line of Python code from the Agent input, evaluates the code and computes the result, prints the result to the Agent, and repeats the process until the Agent exits, making it ideal for rapid experimentation and debugging. Additionally, the generated code is saved as a file for future modification and reproduction, offering users greater flexibility in their analysis.

The agent can automatically read the local data structure and correct errors in the code. Here we provide an example:

Query: Calculate the frequency of the mouse changing from Standing to Walking.

```
1 # 1st try:
2
3 import pandas as pd
4
5 data = pd.read_csv('workspace/user_logs/240919
6 _135012_6e636df89a7e43f4afd5b2d2cb9773e4/cluster.csv/result.csv')
7 data.head()
```

**Listing 3** Python Example

Python output:

```
NotADirectoryError(20, 'Not a directory')
```

Agent Responds:

It seems there was an error because the path provided is not a directory. Let's correct the path and try again. I'll read the CSV file and inspect its contents to understand its structure.

```

1 # 2nd try:
2
3 import pandas as pd
4
5 # Correcting the path and reading the CSV file
6 data = pd.read_csv('workspace/user_logs/240919
   _135012_6e636df89a7e43f4afd5b2d2cb9773e4/cluster.csv')
7
8 # Displaying the first few rows of the dataframe to understand its structure
9 print(data.head())

```

Listing 4 Python Example

Python output

frame_id	behavior
0	0 crouched
1	12 standing
2	24 walking
3	36 walking
4	48 walking

Agent Responds:

The data has been successfully read. The structure of the dataframe is as follows:

frame_id	behavior
0	crouched
12	standing
24	walking
36	walking
48	walking

Now, let's calculate the frequency of the mouse changing from "standing" to "walking".

```

1 # 3rd try:
2
3 # Calculate the frequency of transitions from 'standing' to 'walking'
4
5 # Shift the behavior column to compare current and next behavior
6 data['next_behavior'] = data['behavior'].shift(-1)
7
8 # Filter the transitions from 'standing' to 'walking'
9 transitions = data[(data['behavior'] == 'standing') & (data['next_behavior'] == '
   walking')]
10
11 # Calculate the frequency
12 frequency = len(transitions)
13
14 print(f'The frequency of transitions from standing to walking is: {frequency}')

```

Listing 5 Python Example

Python output

The frequency of transitions from standing to walking is: 342

Agent Responds:

The frequency of transitions from "standing" to "walking" is: \*\*342\*\*.

If you need any further analysis or have additional questions, feel free to ask!

## 4.7 Evaluation of MouseGPT Model

### *Comparison with other language models*

We compared MouseGPT-Large, and MouseGPT-Lite, with InternVL2, MiniCPM, and GPT-4o, using a carefully selected test set (Extended Fig. 5).

First, we performed inference on all test sets using each model (Extended Fig. 3a). Then, we involved 15 senior researchers in animal behavior to evaluate the results based on human expertise. The evaluation was conducted through two methods, with the reviewers being blind to the identity of the models being reviewed. The first method involved a **correctness evaluation**, where researchers were shown an image, a prompt containing speed information, and the model’s output. They were asked to assess whether the output was ‘correct’ or ‘incorrect’ based on three criteria: (1) whether there were factual errors, (2) whether the formatting adhered to the specified requirements, and (3) whether there was unnecessary repetition.

The second method involved a **side-by-side model comparison** (Extended Fig. 3b), where the reviewers were provided with the inputs to the models and the outputs from two different models, selecting the better result based on (1) factual correctness and formatting, (2) whether the terminology used matched industry standards, and (3) the level of detail in describing the behavior.

To ensure the consistency of the evaluation, we provided some repeated questions to different reviewers. The results indicated that the reviewers’ responses were consistent, demonstrating a high level of agreement in their evaluations.

### *Evaluation of Behavioral Phenotype Prediction*

We evaluated the Behavioral Phenotype Prediction results by comparing the predictions made by the model with the actual behavioral phenotypes of the mice. Since the output format from the LLM is not predefined, the model typically generates text representing its prediction, which we then interpret and standardize for consistency. We manually adjusted the format of the LLM’s output to align with the correct prediction format, ensuring uniformity. In cases where the model encountered runtime errors (e.g., failure to generate code or incomplete output), we re-executed the process. To assess the model’s performance, we computed the accuracy and F1-score based on the predictions from the selected test set, providing a quantitative evaluation of the model’s ability to accurately predict the behavioral phenotypes.

## Declarations

**Acknowledgements.** This work was supported by The National Natural Science Foundation of China grant 32192410, 32192414, 32330043, STI2030-Major Projects (2021ZD0203900), The National Natural Science Foundation of China 82371522, The National Natural Science Foundation of China grant 32171025, ShanghaiTech AI4S Initiative SHTAI4S202404, HPC Platform of ShanghaiTech University, ShanghaiTech GenAI Project, The Library and Office of IT Services of ShanghaiTech University, National Key R&D Program of China (2022YFF0902301), NSFC programs (61976138, 61977047), STCSM (2015F0203-000-06), and SHMEC(2019-01-07-00-01-E00003). We also acknowledge support from Shanghai Frontiers Science Center of Human-centered

Artificial Intelligence (ShangHAI), Shanghai clinical research and trail center, Shanghai Frontiers Science Center for Biomacromolecules and Precision Medicine, and MoE Key Lab of Intelligent Perception and Human-Machine Collaboration (ShanghaiTech University).

**Competing interests.** The authors declare no competing interests.

**Ethics approval and consent to participate.** All experiments procedures were approved by the Institutional Animal Care and Use Committee (IACUC) of ShanghaiTech University.

**Data Availability.** All data used in this study will be made publicly available in a relevant repository following publication. The preview dataset is available upon request. This includes the full-resolution videos with all eight views, the corresponding pre-processed image sequences, and frame-level data such as Query Prompts, Kinematic Information, and Open-vocabulary Behavior Descriptions generated by different models, with a total data volume exceeding 20 TB. Additionally, we will provide all weights for models proposed in this paper: MouseGPT-Large, MouseGPT-Lite, and the Kinematic Estimation Models.

**Code Availability.** The software developed for this study will be open-sourced and freely accessible after publication. The Code preview is available upon request. Comprehensive installation and usage tutorials will be provided. MouseGPT will be open-sourced to the community and licensed under the CC BY-NC-ND 4.0 license. To ensure the reproducibility of the results presented in this paper, we will also share all intermediate results along with their corresponding code.

**Author Contribution.** J.Y. and J.H. conceived the project and T.X., Y.W., P.Y. designed the experiments. T.X., Y.W. and T.Z. designed and implemented the algorithm and trained the models. P.Y., S.T. collected and check data and Z.T., X.C., H.L. assisted. K.S., T.Z. processed the raw videos and computed the coordinate of 3D skeleton. H.W. and X.W. support the psychedelics in this study. S.T., P.Y. and T.Z. performed the analysis for hallucination behavior. Y.L., Y.W., Z.T. and P.Y. evaluate the performance of different VLMs. T.X., Y.W., P.Y., T.Z., K.S., S.T., and Y.L. participated in the writing of the corresponding content in the manuscript and J.W., J.H. and J.Y. revised the manuscript. J.H. and J.Y. supervised the project.